NASA Contractor Report 163121

NASA-CR-163121
19820013324

OPTIMIZATION OF THRUST ALGORITHM CALIBRATION

for

THRUST COMPUTING SYSTEM (TCS) FOR THE NASA HIGHLY MANEUVERABLE AIRCRAFT TECHNOLOGY (HiMAT) VEHICLE'S PROPULSION SYSTEM

M. J. Hamer and R. I. Alexander

NASA

National Aeronautics and
Space Administration

December 1981

NF02067

FINAL REPORT

OPTIMIZATION OF THRUST ALGORITHM CALIBRATION

FOR

THRUST COMPUTING SYSTEM (TCS) FOR THE NASA HIGHLY MANEUVERABLE AIRCRAFT TECHNOLOGY (HiMAT) VEHICLE'S PROPULSION SYSTEM

A011/FR

SUBMITTED TO

CANADIAN COMMERCIAL CORPORATION

FOR

NASA DRYDEN FLIGHT RESEARCH CENTER POST OFFICE BOX 273 EDWARDS, CALIFORNIA 93523

DECEMBER 1981

NASA

National Aeronautics and
Space Administration

FOREWORD

This Final Report is submitted in fulfillment of the requirements of Article IV of NASA Contract NAS4-2812, Canadian Commercial Corporation Contract 1PD.70E5-80-1, SN 7PD80-00101. The work was conducted under the direction of the HiMAT Project Office, NASA/DFRC, Edwards AFB, California. The cognizant propulsion engineer was Mrs. J.L. Baer-Riedhart, NASA/DFRC.

Altitude facility data were provided from tests conducted at NASA Lewis Research Center. Mr. L.A. Burkardt was the NASA project engineer (analysis).

The optimization of the thrust algorithm calibration was conducted by Computing Devices Company, Propulsion Systems Group. Mr. M.J. Hamer was the project engineer and performed the analysis in conjunction with Mr. R.I. Alexander.

LIST OF SYMBOLS

A   area

A57   approximate value of algorithm calibration
             coefficient C67

b   bias error

C56   algorithm calibration coefficient

C67   algorithm calibration coefficient

E   algorithm calibration coefficient

f( )   functional relationship

F_{GC} computed gross thrust

F_{GM} facility measured gross thrust

KMODE   engine control mode signal

M   Mach number

PLA   power lever angle

P_S static pressure

P_T total pressure

s   precision error

T_T total temperature

U   total uncertainty

X $= \gamma M^2$

γ ratio of specific heats

δ pressure correction to sea level

σ standard deviation

Subcripts:

C   casing

E   estimated value

L   liner

n   new value

Stations:

O   free stream

others   see figure 2

INTRODUCTION

BACKGROUND

In-flight gross thrust computation is a continuing task for all agencies concerned with the development and test of aircraft. Computing techniques usually fall into the categories of direct force measurement, internal or gas generator calibration, and nozzle exit pressure traversing. The gross thrust computing technique developed by Computing Devices Company (ComDev) is a simplified internal one that uses a flow calibration of the engine tailpipe alone.

SIMPLIFIED THRUST COMPUTING TECHNIQUE. The simplified technique uses measured total and static pressures in the engine tailpipe and ambient static pressure to compute gross thrust. The equations are based on a one-dimensional analysis of the flow. The gas flow model accounts for friction, heat and mass transfer, and three-dimensional effects through the use of empirically-determined calibration coefficients. Instrumentation bias may also be eliminated by calibration.

Gas generator methods for computing thrust require many engine measurements, comprehensive analytical or model work and extensive full-scale calibration testing. The simplified technique requires fewer and simpler engine measurements and computing requirements are negligible in comparison to gas generator methods. Thrust may be processed on-line in the aircraft without compromising accuracy. As a result, the simplified technique is considered to be suitable for flight test and for use on production engines.

The technique was originally developed using ground level engine data on the J85-CAN-15 afterburning turbojet engine [1]. The method was later extended to two afterburning turbofan engines (TF30, F100) using NASA altitude facility data. The turbofan results [2] evaluated the technique over a wide range of Mach/altitude test conditions. The F100 system accuracy was verified on a second engine without altering the calibration of the algorithm. The results were employed in-flight on a NASA F-15 test aircraft with an accuracy comparable to the engine manufacturer's gas generator method [3].

HiMAT EVALUATION PROGRAM

OBJECTIVE. The thrust computing system (TCS) for HiMAT is being jointly developed by NASA and ComDev with an objective to produce a system which will provide optimum accuracy for the computation of in-flight gross thrust of the HiMAT engine over the operational envelope during all steady-state modes of operation.

SCOPE. Under previous [4] NASA Contract NAS4-2644, ComDev provided engine pressure instrumentation design, manufacture and installation, system error analysis, and a preliminary gross thrust algorithm. Approximate values of the algorithm calibration coefficients were obtained by using engine pressures and thrust values from the J85-GE-21 model specification, and pressure ratios from previous J85-CAN-15 experience. The preliminary algorithm was used to estimate pressure transducer ranges and system sensitivity to pressure measurement errors prior to final calibration of the system using altitude facility testing.

The current HiMAT work is discussed in this Report and uses altitude facility test data on one J85-GE-21 engine in order to optimize the gross thrust algorithm calibration coefficients. This work is considered significant for three major reasons: 1) it allows the afterburning turbojet algorithm to be evaluated over the engine envelope (previous J85 work was based on ground level data only), 2) the HiMAT engine was operated using different engine control schedules so that the simplified technique's accuracy can be evaluated with change in exhaust nozzle schedules (this work was recommended in [2]), and 3) the current HiMAT work investigated casing as well as liner static pressure taps. Previous ground level J85 tests used casing static pressure taps only. Finally, the current results are presented in such a way that the reader can assess the method's accuracy for a calibration based on data from one test condition versus the accuracy for a calibration based on several flight test conditions. The final gross thrust algorithm was delivered to NASA as a FORTRAN subroutine.

ENGINE DESCRIPTION

The HiMAT ground test engine is a J85-GE-21 afterburning turbojet, S/N 225326, equipped with a standard bill-of-materials (BOM) control system. The engine's aft sections were modified for installation of the TCS hardware. The modifications were: 1) installation of total pressure rakes in the center-cone support body, 2) installation of static pressure taps in the afterburner casing and afterburner liner aft of the afterburner flameholders, 3) installation of static pressure probes at the nozzle inlet replacing the respective stand-off bolts, and 4) installation of harnesses and tubing for transferring the pneumatic signals to an engine-mounted bulkhead at the compressor case. For engine operation requiring off-design exhaust nozzle scheduling, a separate throttle signal was sent to the afterburner fuel controller, which also controls the nozzle area, to command the nozzle to the desired area schedule.

ALTITUDE TEST FACILITY

A photograph of the J85-GE-21 engine installed in the NASA Lewis PSL3 altitude facility is shown in figure 1. The station locations and the instrumentation used in the facility are shown in figure 2. The facility had a calibrated load cell thrust bed for determining actual gross thrust.

NASA provided estimates of bias error, precision error and total uncertainty for the facility measurement of gross thrust. The bias error is a constant 49N and was estimated from data system and instrumentation specifications. The precision error varies as a function of altitude and power setting and represents the standard deviation of 40 consecutive data scans at a given test condition. Total uncertainty was calculated according to the method in [5]. For simplification the results were plotted as a function of thrust level as shown on figure 3. The total uncertainty, through the precision error component, contains a contribution due to engine thrust fluctuations at a fixed power setting. As a result, this total uncertainty represents a conservative estimate of the facility thrust measurement accuracy. The actual facility accuracy lies between the bias limit and total uncertainty plotted on figure 3.

ENGINE INSTRUMENTATION

The engine instrumentation kit produced for the J85-GE-21 HiMAT engine was adapted from a previous design used on J85-GE-5

and J85-CAN-15 engines which have accumulated in excess of 10,000 flight hours. Total pressure is measured by four, three-probe rakes at the turbine exit (designated P_{T5}). Static pressure is measured in the afterburner flameholder region both on the liner (P_{S6L}) and on the casing (P_{S6C}) each with 4 pressure taps. Static pressure is measured on the liner at the nozzle entry region (P_{S7}) using 4 pressure taps which replace liner stand-off bolts. Engine tailpipe measurement stations are shown on figure 4. At each station the pressures are manifolded to provide a pneumatic average, and routed (using 0.32 cm outside diameter tubing) to an outlet bracket mounted on the compressor case. The low profile of the pneumatic plumbing did not interfere with the installation of the engine in the vehicle.

The detailed design of the pressure probes for P_{T5}, P_{S6C} and P_{S7} remained unchanged from that used on the J85-GE-5 and J85-CAN-15 engines. For the HiMAT program, a new liner tap for station 6 was designed, ground tested, and used during the altitude testing. A photograph of the new liner tap design is shown in figure 5. The detailed design of all of the probes is given in [4].

The pressure probe and manifold axial and circumferential exact locations are shown on figure 6. Separate manifolds were used at station 6 to measure P_{S6C} and P_{S6L}. Ambient static pressure was determined from nozzle exit external static taps as shown.

NASA provided estimates of bias error, precision error and total uncertainty for the pressure transducers used for measuring P_{T5}, P_{S6L}, P_{S6C}, P_{S7} and P_{S0}. The bias error is a constant 0.023 N/cm^2 for P_{T5}, P_{S6L}, P_{S6C} and P_{S7} and a constant 0.007 N/cm^2 for P_{S0}. The bias errors were estimated from data system and instrumentation specifications. The precision error varies as a function of altitude and power setting and represents the standard deviation of 40 consecutive data scans at a given test condition. For simplification, the results were plotted as a function of pressure level as shown on figure 7. Since the total uncertainty contains a contribution due to engine pressure fluctuations at a fixed power setting, the actual pressure measurement accuracy lies between the bias limits and total uncertainty limits shown on figure 7.

An additional set of pressure transducers for the TCS was supplied by NASA Dryden. The NASA Lewis transducers were found to be more repeatable and accurate during the altitude tests, therefore, they were used as the primary instrumentation. A comparison of the two sets of transducers was made and is shown in Appendix B.

TEST CONDITIONS

The conditions for the standard nozzle test and open-sched-
uled nozzle test are illustrated in figure 8. Table 1 lists
these conditions including the power range for each test. All
of the test conditions were at standard day temperature except
for the Mach 0.4, 6100 m condition which was approximately 25°C
hotter than standard. As shown, the engine was tested over a
wide range of conditions including the extremes of the standard
day engine envelope. The engine was tested with a clean inlet
configuration (no distortion screens). The general test proce-
dure was to establish the facility flow on a given Mach/altitude
test condition. Once the engine was established (4 minutes) at
each throttle setting, a data point was taken followed by a re-
peat data point (1/2 minute later).

The standard nozzle schedule and open nozzle schedule are
shown on figure 9 for power lever angles from idle (0-13 degrees
PLA) to military power (90-93 degrees PLA). In the open mode,
the engine exhaust gas temperature control at military power is
downtrimmed by approximately 110°K and nozzle area is opened up
by approximately 13%. At each test condition in the standard
mode, typically 5 non-afterburning and 3 afterburning power set-
tings were tested. In the open mode, only non-afterburning pow-
er settings were tested.

DATA REDUCTION

INTRODUCTION

The engine batch data were received from NASA Lewis and were reduced to examine the consistency between the measured tailpipe ratios and between pressure ratio and facility gross thrust. This was done to identify any outliers in the data prior to calibration of the simplified gross thrust algorithm.

DATA BASE

Measured tailpipe pressures P_{T5}, P_{S6L}, P_{S6C}, P_{S7} and P_{S0} and facility thrust F_{GM} were examined. This was done for all of the operating points, a total of 388 data points including the repeat points.

BEHAVIOUR OF TAILPIPE PRESSURES

Typical values of the J85-GE-21 tailpipe pressures are shown in figure 10 to show their general behaviour. The standard mode pressures are plotted as a function of power setting for the 0.9, 7620 m test condition. The pressures increase in going from flight idle to a maximum near military power. P_{T5} and P_{S6L} remain constant throughout afterburning. P_{S6C} drops slightly with degree of afterburning while P_{S7} decreases markedly with degree of afterburning.

TAILPIPE PRESSURE DIAGNOSTICS

Liner pressure ratio P_{S6L}/P_{T5} was plotted as a function of P_{S7}/P_{T5} as shown on figure 11. The data were found to be very consistent, particularly in non-afterburning, over the full operating envelope. Only three data points out of the 388 were identified as measurement outliers, based on a three-sigma limit, and were eliminated. All three occurred at flight idle in the top left-hand portion of the envelope. As shown on figure 11, the non-afterburning data points for both engine control modes collapse to a straight line with a spread of ±0.57 per cent of the point at the 2-sigma level. The afterburning data also collapse to a straight line and the spread is ±1.81 per cent of the point at the 2-sigma level.

Casing static pressure ratio P_{S6C}/P_{T5} was also plotted as a function of P_{S7}/P_{T5} as shown on figure 12. These data were also found to be very consistent, with no measurement outliers found. As shown on figure 12, the non-afterburning data

6   A011/FR

collapse to a straight line with a spread of ± 0.85 per cent of the point at the 2-sigma level (versus ± 0.57 per cent of the point for the liner data). The afterburning data, collapsed to within ± 1.27 per cent of the point (versus ± 1.81 per cent of the point for the liner data). Compared to liner data, the casing data were less consistent in non-afterburning and more consistent in afterburning.

THRUST VS PRESSURE DIAGNOSTIC

To identify any outliers in the measured gross thrust data, facility corrected gross thrust, F_{GM}/δ, was plotted as a function of pressure ratio P_{T5}/P_{S0} as shown on figure 13. No outliers in the measured thrust data were found. As shown on figure 13, the non-afterburning data points for both engine control modes collapse to a straight line with a spread of ± 4.3 per cent of the point at the 2-sigma level. Afterburning data could not be checked in this manner since a single correlation between thrust and P_{T5}/P_{S0} does not exist.

ACCURACY PREDICTIONS

Accuracy predictions in the next section were based on the bias error (b) and twice the precision error (2s) of the data. These errors were then combined using the method in [5] to produce a total uncertainty (U) of the algorithm, which includes test stand uncertainty.

$$U = |b| + 2s$$

ALGORITHM CALIBRATION RESULTS

FINAL GROSS THRUST ALGORITHM

The equations used in the final gross thrust algorithm are summarized below. Derivations of the basic equations are given in [1]. The algorithm is shown schematically in figure 14.

ENGINE DATA REQUIRED. The following engine geometrical data are specified:

$$CA7 = A_7$$

CALIBRATION COEFFICIENTS. The following calibration coefficients are determined by engine calibration, and their numerical values are supplied to the gross thrust algorithm:

$$C56, \; A57, \; C6A, \; C6B, \; C6C, \; EA, \; EB$$

An appropriate average value (γ) for the ratio of specific heats of the exhaust gas is also defined during calibration.

MEASUREMENTS. The following pressure measurements are required within the engine tailpipe:

$$P_{T5}, \; P_{S6L}, \; P_{S7}$$

Ambient static pressure is also required:

$$P_{S0}$$

If the engine is operating in a non-standard control mode, alternate values of A57, C6A, C6B, C6C, EA and EB may be selected using the KMODE signal.

CALCULATIONS. The following calculations are required to determine the gross thrust.

(a) Calibration coefficient E is calculated from:

$$E = EA.P_{S6} + EB$$

and is used to modify the measured value of P_{S7} to form a new value, P_{S7n}:

$$P_{S7n} = f(P_{S7}, \; E)$$

(b) P_{T6} is calculated following the approach in [1]:

$$P_{T6} = f(P_{T5}, P_{S6}, C56, \gamma)$$

(c)   The calibration procedure provided a relationship between $C67$ and an estimated value of A_8/A_7, $(A_8/A_7)_E$.

$$C67 = C6A \cdot (A_8/A_7)^2_E + C6B \cdot (A_8/A_7)_E + C6C$$

This was done to obviate the need for iteratively computing $C67$ as a function of the final computed value of A_8. $(A_8/A_7)_E$ is first determined from an estimated value of X_7, X_{7E}, using the isentropic flow relation:

$$(A_8/A_7)_E = f(X_{7E}, \gamma)$$

where X_{7E} is determined using a combination of the isentropic flow relation:

$$X_{7E} = \gamma M_7^2 = \frac{2\gamma}{\gamma - 1}\left[\left(\frac{P_{T7}}{P_{S7n}}\right)^{\frac{\gamma - 1}{\gamma}} - 1\right]$$

and the following equation, which uses an approximate value of $C67$ (= $A57$), to first calculate P_{T7}:

$$P_{T7} = f(P_{T6}, P_{S7n}, A57, \gamma)$$

The approximations in this step are absorbed in the calibrated relationship for $C67$ as a function of $(A_8/A_7)_E$.

(d) X_6 is calculated using the isentropic flow relation:

$$X_6 = \gamma M_6^2 = \frac{2\gamma}{\gamma - 1}\left[\left(\frac{P_{T6}}{P_{S6}}\right)^{-1} - 1\right]$$

(e) X_7 is calculated using the exact value of $C67$ following the approach in [1]:

$$X_7 = f(P_{S6}, X_6, P_{S7n}, C67)$$

(f) P_{T7} is calculated using the isentropic flow relation:

$$P_{T7} = P_{S7n}\left[1 + \frac{\gamma-1}{2\gamma} X_7\right]^{\frac{\gamma}{\gamma-1}}$$

and $P_{T8} = P_{T7}$ (assumed). This assumption is absorbed by the calibration coefficients.

(g) P_{T8}/P_{S0} is calculated to check for choking. For choked flow, defined by

$$\frac{P_{T8}}{P_{S0}} \geqslant \left[\frac{(\gamma+1)}{2}\right]^{\frac{\gamma}{\gamma-1}}$$

gross thrust is calculated using the final thrust equation in [1] for choked flow:

$$F_G = f_1(P_{S7n}, X_7, A_7, P_{S0}, \gamma)$$

(h) If the flow is unchoked, gross thrust is calculated using the final thrust equation in [1] for unchoked flow:

$$F_G = f_2(P_{S7n}, X_7, A_7, P_{S0}, \gamma)$$

The preliminary algorithm [4] was calibrated using data at the Mach 0.9, 7620 m altitude test condition. This provided reasonable accuracy over the flight envelope. A significant improvement in accuracy was made by recognizing that one of the coefficients (E) varied as a linear function of tailpipe pressure level. As a result, the preliminary algorithm was modified accordingly. Other revisions included the capability to use separate sets of calibration constants for each engine control mode (KMODE) and removing the requirement for having an afterburner check [6].

ALGORITHM CALIBRATION

The HiMAT thrust algorithm (HIMATF) was calibrated on each of 7 sets of HiMAT J85-GE-21 engine pressure data and NASA Lewis measured thrust and ambient pressure. The seven sets of data were collected at the following conditions:

Mach = 0.9, 7620 m altitude, standard and open nozzle modes, liner P_{S6} taps

Mach = 0.9, 7620 m altitude, standard nozzle mode, liner P_{S6} taps

Mach = 0.9, 7620 m altitude, open nozzle mode, liner P_{S6} taps

All Mach/altitudes, standard and open nozzle modes, liner P_{S6} taps

All Mach/altitudes, standard nozzle mode, liner P_{S6} taps

All Mach/altitudes, open nozzle mode, liner P_{S6} taps

All Mach/altitudes, standard nozzle mode, casing P_{S6} taps

The calibration method produced a set of calibration coefficients which enabled the thrust algorithm (HIMATF) to compute a value for thrust which was as close as possible to the measured thrust. The calibration coefficients were then placed in the thrust algorithm and thrust was computed using pressures from a set of data points different from those used to calibrate. This prediction of thrust was compared to the measured thrust. A comparison of the calibration coefficients E and C67 from the seven calibration data sets is shown in figure 15. Figure 16 illustrates the scatter of the calibration coefficient C67 for the seven calibration sets; the scatter being proportional to the accuracy of the thrust algorithm.

CALIBRATION AT ONE MACH/ALTITUDE CONDITION

The HiMAT thrust algorithm was calibrated at the Mach 0.9, 7620 m altitude condition using both repeat and non-repeat data points. Points were deleted when the computed pressure ratio P_{T8}/P_{S0} was less than 1.65 for standard nozzle mode and less than 1.50 for open nozzle mode due to accuracy deterioration of the algorithm at low pressure ratios. Three calibrations were conducted at this Mach/altitude condition and the resulting calibration coefficients are listed in table 2. The first calibration (calibration #1) used both standard mode data at Mach 0.9, 7620 m (runs 1A, 5A, 9A) and open data (runs 10B and 14B) for a total of 59 points. This calibration was used to predict on all Mach/altitude conditions, both standard and open modes,

non-repeat points only. Duplicate runs 1A, 5A and 14B at Mach 0.9, 7620 m and 1B and 5B at Mach 0.6, 9140 m were deleted from the prediction to ensure equal representation of each Mach/altitude condition. Line 1 of table 4 shows the results of this prediction. With a total of 128 points, the average bias error of $(F_{GC}-F_{GM})/F_{GM}$ was -0.16 per cent and twice the precision error was 2.27 per cent where F_{GC} is computed thrust, F_{GM} is Lewis altitude facility measured thrust and precision error is the standard deviation of $(F_{GC}-F_{GM})/F_{GM}$ about the average bias. The bias and precision of $F_{GC}-F_{GM}$ in kN are also given. The 128 predicted points are plotted in figure 17.

Figure 18 and line 2 of table 4 show the results of predicting with calibration #1 on only the standard mode points in line 1. The number of points decreased to 93, the bias error changed to -0.29 per cent and twice the precision error decreased to 2.18 per cent. The prediction on open mode data only is plotted in figure 19 and is summarized in line 3 of table 4. For 35 points, bias error was 0.21 per cent and twice the precision error was 2.39 per cent.

Calibration #2 was obtained by calibrating on only the standard mode points from Mach 0.9, 7620 m used in calibration #1. Line 4 of table 4 shows the prediction using calibration #2 on the set of standard mode data only from all Mach/altitude conditions used in the line 2 prediction. The results of this prediction are shown in figure 20. Compared to line 2, bias error remained about the same at -0.31 per cent but twice the precision error improved to 1.83 per cent. When only open mode data from Mach 0.9, 7620 m were used to calibrate (calibration #3, line 5, table 4) there were only 17 data points available, possibly explaining the prediction results (figure 21) on the 35 open mode data points from all Mach/altitudes. Compared to line 3 of table 4, where both modes with a total of 59 points were used to calibrate, the bias error increased to 0.26 per cent and twice the precision error increased to 2.44 per cent.

CALIBRATION AT ALL MACH/ALTITUDE CONDITIONS

The HiMAT thrust algorithm was calibrated on data from all Mach/altitude conditions using only repeat points and deleting all points for which the computed pressure ratio P_{T8}/P_{S0} was less than 1.65 for standard mode and less than 1.50 for open mode. The calibration coefficients for the three calibrations conducted at all Mach/altitudes are listed in table 2. The calibration coefficients for the calibration using the casing data are also shown and are discussed below. The first calibration (calibration #4) used both standard and open mode data with runs 1A, 5A, 1B, 5B and 14B deleted. Points having P_{T8}/P_{S0}

less than 1.65 for standard and less than 1.50 for open mode were also deleted leaving a total of 123 points. This calibration was used to predict on a set of data similar in all respects to the calibration set with the exception that only non-repeat points were used. This prediction is described in line 1 of table 5 and the results are shown in figure 22. For a total of 128 predicted points, bias error was -0.16 per cent and twice the precision error was 2.10 per cent. Comparing this line to line 1 of table 4 shows that prediction accuracy improves slightly when more conditions are used to calibrate. Twice the precision error decreased from 2.27 per cent in table 4 to 2.10 per cent in table 5. The bias error change between the two predictions was negligible.

When calibration #4 was used to predict on only the standard mode data of line 1, table 5, the bias error changed to -0.20 per cent and twice the precision error decreased to 1.97 per cent for a total of 93 points. Line 2 of table 5 and figure 23 show the results of this prediction. The small reduction in precision error and bias error resulting from calibrating on several Mach/altitude conditions instead of only one is again evident when line 2 of table 5 is compared to line 2 of table 4. Bias error decreased from -0.29 per cent to -0.20 per cent and twice the precision error decreased from 2.18 per cent to 1.97 per cent.

Predicting on only the open mode data in line 1 of table 5 produced a bias error of -0.06 per cent and twice the precision error of 2.43 per cent for a total of 35 points. These results are illustrated in figure 24 and line 3 of table 5.

The second calibration at all Mach/altitude conditions (calibration #5) used only standard mode data from line 1 of table 5. A total of 87 points were included in this calibration. When this calibration was used to predict on the same standard mode data as in lines 1 and 2 of table 5, the resulting bias error was -0.20 per cent and twice the precision error was 1.68 per cent. (See figure 25 and line 4 of table 5.) The improvement in precision error resulting from specializing on engine operating mode is shown by comparing line 4 with line 2 of table 5. Twice the precision error decreased from 1.97 per cent to 1.68 per cent. Calibrating on several Mach/altitude conditions instead of one decreased twice the precision error slightly, on prediction, from 1.83 per cent to 1.68 per cent as shown in line 4 of table 4 and line 4 of table 5.

The third calibration at all Mach/altitude conditions (calibration #6) used only open mode data from line 1 of table 5. Figure 26 and line 5 of table 5 show the results when calibration #6 was used to predict on all the same open mode points as

in lines 1 and 3 of table 5. The bias error for the 35 points was 0.06 per cent and twice the precision error was 2.24 per cent.

Tables 4 and 5 show that using data from several Mach/altitude conditions to calibrate results in slightly better predictions on all Mach/altitude data than if data from only one condition is used to calibrate. Calibrating on data from one condition, both modes and predicting on all conditions, both modes produced a bias error of -0.16 per cent and twice the precision error of 2.27 per cent, whereas calibrating on all conditions, both modes and predicting on all conditions, both modes produced a bias error of -0.16 and twice the precision error of 2.10 per cent. Similarly, calibrating on only standard mode data at one condition and predicting on only standard mode data at all conditions produced a bias error of -0.31 per cent and twice the precision error of 1.83 per cent, while a calibration on all conditions produced a prediction bias error of -0.20 per cent and twice the precision error of 1.68 per cent.

Optimum accuracy of the HiMAT thrust algorithm over the engine envelope is demonstrated in line 4 of table 5 for standard mode operation. The algorithm was calibrated using data from all Mach/altitude test conditions, standard mode only. Bias error (b) was -0.20 per cent and twice the precision error (2s) was 1.68 per cent. These errors were combined using the method in [5] to produce an algorithm total uncertainty (U) of 1.88 per cent of the point, which includes altitude facility test stand uncertainty.

$$U = |b| + 2s$$

Line 5 of table 5 shows optimum algorithm accuracy for open mode operation. The algorithm was calibrated using data from all Mach/altitude test conditions, open mode only. Bias error was 0.06 per cent and twice the precision error was 2.24 per cent. Therefore, the total uncertainty of the algorithm including test stand uncertainty for open mode operation is 2.30 per cent of the point.

CALIBRATION ON OPEN MODE COMPARED TO NORMAL MODE

Calibrations were produced for standard and open mode data together, only standard mode data and only open mode data. Calibrating on both modes using one test condition and predicting on standard mode data produced twice the precision error of 2.18 per cent while calibrating on only standard mode data and

predicting on standard mode data produced twice the precision error of 1.83 per cent. Table 5 shows that when the calibrations used data from several Mach/altitude conditions the predictions again were better when the operating mode was specialized. Calibrating on only standard mode data and predicting on standard mode data produced twice the precision error of 1.68 per cent instead of the 1.97 per cent resulting from the calibration on both modes. Similarly, an open mode calibration predicting on open mode data produced twice the precision error of 2.24 per cent instead of the 2.43 per cent resulting from the calibration on both modes.

CASING TAP DATA COMPARED TO LINER TAP DATA

At engine station 6, static pressure was measured both at the afterburner liner surface and in the space between the liner and the casing. Figure 27 compares casing with liner P_{S6} at each test condition, standard mode. Figure 28 compares the same casing with liner P_{S6} data in a normalized manner. At maximum afterburning, casing P_{S6} approximately equals liner P_{S6} but at lower power settings, casing P_{S6} is up to 7 per cent higher than liner P_{S6}. Figure 29 shows that in the open mode, casing P_{S6} varies up to 10 per cent above liner P_{S6}.

Casing P_{S6} pressures were used to calibrate the thrust algorithm at all Mach/altitude conditions, standard mode. The difference between liner and casing calibrations is evident in table 2 and in figure 15 in which the higher level and more negative slope of the casing C67 curve can be seen. The variable calibration coefficient E is also higher for casing than for liner pressures. The casing calibration was used to predict on casing pressure from all Mach/altitude, standard mode data. Figure 30 and line 6 of table 5 show that the prediction bias error was -0.26 per cent and twice the precision error was 3.10 per cent for 93 points. Similar calibration and prediction (line 4, table 5) using liner P_{S6} data produced twice the precision error of only 1.68 per cent.

THRUST ALGORITHM SENSITIVITY TO PRESSURE MEASUREMENT ERROR

The sensitivity of the HiMAT thrust algorithm (HIMATF) to errors in the measurement of pressures P_{S0}, P_{S6}, $P_{T5}-P_{S6}$, $P_{T5}-P_{S7}$ (HiMAT flight transducer configuration) was calculated at several conditions. Sensitivities at the two power settings, military and maximum afterburning, were investigated for sea-level-static and six other Mach/altitude conditions covering the HiMAT engine operating envelope.

TRANSDUCER RANGES OF THE DRYDEN SYSTEM. Ambient static air pressure, P_{S0}, is obtained from the aircraft data system and has a range of 0 to 13.8 N/cm^2. Afterburner static pressure in the flameholder region, P_{S6}, is measured by an absolute pressure transducer with a range of 0 to 34.5 N/cm^2. The tailpipe pressure differential, $P_{T5}-P_{S6}$, is measured by a differential pressure transducer with a range of 0 to 10.3 N/cm^2. The second differential pressure transducer, $P_{T5}-P_{S7}$, also has a range of 0 to 10.3 N/cm^2. Table 6 lists the transducer ranges.

THRUST ALGORITHM SENSITIVITY. Table 7 lists the 7 Mach/altitude conditions and the change in computed thrust resulting from errors in the measurement of each pressure. The assumed pressure measurement errors are ±0.25 per cent of full scale for P_{S0} and ±0.33 per cent of full scale for P_{S6}, $P_{T5}-P_{S6}$ and $P_{T5}-P_{S7}$. The thrust change was determined by computing thrust with the unperturbed pressures, and then perturbing one pressure by the amount of the measurement error and recomputing thrust. The change in thrust represents the thrust error resulting from the pressure measurement error for that particular pressure. This is done for all four pressures and the results are root-sum-squared to produce the estimated thrust change due to pressure measurement errors in all transducers.

Therefore at military power, standard day sea-level static conditions, pressure measurement errors of $\pm0.25\%$ of full scale for P_{S0} and ±0.33 per cent of full scale for P_{S6}, $P_{T5}-P_{S6}$ and $P_{T5}-P_{S7}$ produce a computed thrust change of ±0.80 per cent of the point. At intermediate afterburning (PLA $= 110°$) the thrust change reduces to ±0.71 per cent of the point. At Mach 0.9, 7620 m altitude, standard day, the military power thrust change is ±1.06 per cent of the point and the maximum afterburning change is ±0.78 per cent of the point. The Mach/altitude condition at which the thrust algorithm is most sensitive to pressure measurement error is Mach 0.9 at 15240 m, where military power thrust change is ±3.19 per cent of the point and maximum afterburning thrust change is ±2.32 per cent of the point.

The thrust changes resulting from pressure measurement errors are plotted in Figures 31, 32 and 33 for three Mach/altitude conditions for pressure measurement errors from 0 to 0.5 per cent of full scale.

CONCLUSIONS

1. The simplified gross thrust algorithm was evaluated for the J85-GE-21 engine using altitude facility data. Computed thrust values were compared to measured thrust values. The algorithm was found to be very accurate over the engine envelope for both the standard engine mode and the open nozzle mode.

2. The difference in the algorithm accuracy for a calibration based on data from one test condition is small compared to a calibration based on data from all of the test conditions.

3. The algorithm accuracy is slightly improved when the calibration is optimized for each of the standard and open nozzle engine operation modes.

4. Greater accuracy was obtained using liner static tap data than using casing static tap data when optimum accuracy over the range of power settings is required.

5. The algorithm based on the calibration set using all Mach/altitude test conditions for the standard mode produced the optimum accuracy (total uncertainty) over the engine envelope for this mode which was 1.88 per cent of point.

6. The optimum accuracy (total uncertainty) for the open nozzle mode was the result of the algorithm based on the all Mach/altitude open nozzle calibration set and was 2.30 per cent of point over the engine envelope.

RECOMMENDATIONS

1. For cost effectiveness, the method could be calibrated using repeat runs from one Mach/altitude condition rather than the same quantity of data from a variety of Mach/altitude conditions.

2. It was reported in [4] that the simplified approach has the potential to provide a ± 2 per cent of the point accuracy system over most of the flight test envelope. The altitude facility results confirm that with accurate pressure measurement (± 0.33 per cent), the calibration and model error are small enough to produce the desired ± 2 per cent system. In pursuit of this goal, the following are areas for further investigation:

    (a) Optimization of the algorithm accuracy on the HiMAT flight engines to account for any engine-to-engine biases.

    (b) Determination of the accuracy to include installataion effects.

    (c) Comparison of the algorithm based on ground level data only with the algorithm based on Mach/altitude data to predict thrust over the engine envelope.

    (d) Examination of the accuracy of the algorithm using casing tap data for ground level conditions on the three HiMAT engines.

    (e) Development of the HiMAT pressure measurement system to produce a throughput accuracy of ± 0.33 per cent, including transducers, data link and associated interfaces. One method would be to control the transducer environment and use a double transmission scheme [4]. An alternate method would be to preprocess the pressure data before inputting to the data link, and to transmit signals proportional to thrust to the ground-based computer for final processing. These signals could be transmitted with less accuracy than the raw pressure data to achieve ± 2 per cent thrust accuracy.

REFERENCES

1. McDonald, G.B., "Theory and Design of an Airborne Thrust Computing System", prepared under USAF Contract F33657-69-C-0733, August 1974.

2. Hamer, M.J. and Kurtenbach, F.J., "A Simplified Gross Thrust Computing Technique for an Afterburning Turbofan Engine", presented at Society of Flight Test Engineers Ninth Annual Symposium, Arlington, Texas, October 1978.

3. Kurtenbach, Frank J., "Evaluation of a Simplified Gross Thrust Calibration Technique Using Two Prototype F100 Turbofan Engines in an Altitude Facility", NASA Technical Paper 1482, June 1979.

4. Parker, John A., "Thrust Computing System (TCS) for the NASA Highly Maneuverable Aircraft Technology (HiMAT) Vehicle's Propulsion System", R908/FR, Computing Devices Company, April 1980.

5. Abernethy, R.B., et al, "Uncertainty in Gas Turbine Measurements-Handbook", AD-755 356, YU AF AEDC TR 73-5, Arnold Air Force Station, Tennesse, February 1973.

6. "Final Algorithm for In-flight Thrust Computation on the NASA HiMAT J85-GE-21 Engine", User Manual 959322, Computing Devices Company, 25 September 1981.

Run No.	Test condition		Thrust Range (Throttle)	Nozzle Mode
	Mach No.	Altitude (m)		
1A'	0.0	sls	Idle – 110 deg	Standard
1A	0.9	7620	Idle – Max	
1B	0.6	9140	Idle – Max	
2A	0.9	12190	Idle – Max	
2B	0.6	6100	Idle – Mil	
3A	0.9	9140	Idle – Max	
3B	0.9	15240	Idle – Max	
4A	0.6	10670	Idle – Mil	
4B	0.6	3050	Idle – Max	
5A	0.9	7620	Idle – Max	
5B	0.6	9140	Idle – Mil	
6A	1.4	12190	90% – Max	
6B	1.4	13720	90% – Max	
7A	1.2	10670	90% – Max	
7B	1.2	13720	90% – Max	
8A	0.4	3050	Idle – Mil	
8B	0.4	9140	Idle – 90%	
9A	0.9	7620	Idle – Max	
9B	0.6	9140	Idle – Max	Standard Open
10A	0.9	15240	Idle – Mil	
10B	0.9	7620	Idle – Mil	
11A	0.9	9140	Idle – Mil	
11B	0.6	6100	Idle – Mil	
12A	0.6	10670	Idle – Mil	
12B	0.4	9140	Idle – Mil	
13A	0.6	3050	Idle – Mil	
13B	0.4	3050	Idle – Mil	
14A	0.9	15240	Idle – Mil	
14B	0.9	7620	Idle – Mil	
14C	0.0	sls	Idle – Mil	Open
15	0.4	6100	Mil	Standard

Notes: 1. 1A' and 14C are "sea-level-static" tests or as close as PSL3 facility can achieve this condition.

2. 15 is a reference condition used during tests.

Table 1. Test conditions

Calibration No.	1	2	3
Mach/Altitude	0.9/7620 m	0.9/7620 m	0.9/7620 m
Run No.	1A, 5A, 9A, 10B, 14B	1A, 5A, 9A	10B, 14B
Liner or Casing P_{S6}	Liner	Liner	Liner
Mode	Standard and Open	Standard	Open
Number of Points	59	42	17
GAMMA	1.30	1.30	1.30
CA7	227.6	227.6	227.6
A57	-0.19	-0.16	-0.29
C56	0.570	0.570	0.570
EA	0.0011	0.0011	0.0011
EB	-0.0315	-0.0165	-0.0565
C6A	0.38289	0.36943	-0.42567
C6B	-0.48133	-0.58542	0.63516
C6C	-0.07075	0.06723	-0.51846

Table 2. Calibration coefficients (page 1 of 2)

Calibration No.	4	5	6	7
Mach/Altitude	All	All	All	All
Run No.	All except 1A, 5A, 1B, 5B, 14B	All except 1A, 5A, 1B, 5B	All except 14B	All except 1A, 5A, 1B, 5B
Liner or Casing P_{S6}	Liner	Liner	Liner	Casing
Mode	Standard and Open	Standard	Open	Standard
Number of Points	123	87	36	87
GAMMA	1.30	1.30	1.30	1.30
CA7	227.6	227.6	227.6	227.6
A57	-0.19	-0.16	-0.29	0.20
C56	0.570	0.570	0.570	0.570
EA	0.00085	0.00085	0.00110	0.00085
EB	-0.02275	-0.01275	-0.05650	0.02725
C6A	0.33337	0.25997	-0.66251	2.41473
C6B	-0.46175	-0.42871	0.96826	-5.03391
C6C	-0.04189	0.01172	-0.62773	2.49395

Table 2. Calibration coefficients (page 2 of 2)

Run No.	Mach No.	Altitude (m)	Nozzle Mode	Plotting Symbol
1A'	0.0	sls	Standard	
1A	0.9	7620		
1B	0.6	9140		
2A	0.9	12190		
2B	0.6	6100		
3A	0.9	9140		
3B	0.9	15240		
4A	0.6	10670		
4B	0.6	3050		
5A	0.9	7620		
5B	0.6	9140		
6A	1.4	12190		
6B	1.4	13720		
7A	1.2	10670		
7B	1.2	13720		
8A	0.4	3050		
8B	0.4	9140		
9A	0.9	7620		
9B	0.6	9140	Standard Open	
10A	0.9	15240		
10B	0.9	7620		
11A	0.9	9140		
11B	0.6	6100		
12A	0.6	10670		
12B	0.4	9140		
13A	0.6	3050		
13B	0.4	3050		
14A	0.9	15240		
14B	0.9	7620		
14C	0.0	sls	Open	
15	0.4	6100	Standard	

Table 3. Plotting symbols

	Calibration Set (# of Data Points)	Prediction Set (# of Data Points)	Accuracy	
			Bias error, b	Twice the precision error, 2s
			% (kN)	% (kN)
1	Calibration #1 Mach 0.9, 7620m. Standard and open modes. Use 1A, 5A, 9A, 10B, 14B. Repeat and non-repeat points. (59)	All Mach/altitude test conditions. Standard and open modes. Non-repeat points. Use all data except 1A, 5A, 1B, 5B, 14B. (128)	-0.16 (-0.006)	2.27 (0.195)
2	As in 1	As in 1 but standard mode only. (93)	-0.29 (-0.016)	2.18 (0.210)
3	As in 1	As in 1 but open mode only. (35)	0.21 (0.020)	2.39 (0.137)
4	Calibration #2 As in 1 but standard mode only. (42)	As in 1 but standard mode only. (93)	-0.31 (-0.012)	1.83 (0.179)
5	Calibration #3 As in 1 but open mode only. (17)	As in 1 but open mode only. (35)	0.26 (0.014)	2.44 (0.107)

Table 4. Prediction accuracy using calibration data from one test condition
(Mach 0.9, 7620m)

	Calibration Set (# of Data Points)	Prediction Set (# of Data Points)	Accuracy	
			Bias error, b	Twice the precision error, 2s
			% (kN)	% (kN)
1	Calibration #4 All Mach/altitude test conditions. Standard and open modes. Repeat points only. Use all data except 1A, 5A, 1B, 5B, 14B. (123)	All Mach/altitude test conditions. Standard and open modes. Non-Repeat points. Use all data except 1A, 5A, 1B, 5B, 14B. (128)	-0.16 (-0.014)	2.10 (0.172)
2	As in 1	As in 1 but standard mode only. (93)	-0.20 (-0.017)	1.97 (0.185)
3	As in 1	As in 1 but open mode only. (35)	-0.06 (-0.006)	2.43 (0.130)
4	Calibration #5 As in 1 but standard mode only. (87)	As in 1 but standard mode only. (93)	-0.20 (-0.014)	1.68 (0.158)
5	Calibration #6 As in 1 but open mode only. (36)	As in 1 but open mode only. (35)	0.06 (0.000)	2.24 (0.095)
6	Calibration #7 As in 1 but standard mode only. Casing P_{S6}. (87)	As in 1 but standard mode only. Casing P_{S6}. (93)	-0.26 (-0.023)	3.10 (0.290)

Table 5. Prediction accuracy using calibration data from all Mach/altitude conditions

Pressure	Transducer Range (N/cm^2)	ComDev Specified Pressure Measurement Error (% F.S.)
P_{S0}	0 - 13.8	±0.25
P_{S6}	0 - 34.5	±0.33
$P_{T5}-P_{S6}$	0 - 10.3	±0.33
$P_{T5}-P_{S7}$	0 - 10.3	±0.33

Table 6. Pressure transducer ranges

Power Setting	Mach No.	Altitude (m)	Change in computed thrust (% of Point)*				
			P_{S0}	P_{S6}	$P_{T5}-P_{S6}$	$P_{T5}-P_{S7}$	RSS
Mil	0	0	-0.182	0.629	-0.060	0.456	0.800
110° PLA	0	0	-0.188	0.629	0.021	0.275	0.712
Mil	0.9	7620	-0.216	0.668	-0.173	0.781	1.064
Max AB	0.9	7620	-0.237	0.720	0.075	0.182	0.783
Mil	0.6	9140	-0.358	1.069	-0.313	1.282	1.736
Max AB	0.6	9140	-0.383	1.166	0.128	0.291	1.268
Mil	0.9	9140	-0.256	0.769	-0.230	0.949	1.269
Max AB	0.9	9140	-0.281	0.849	0.086	0.208	0.922
Mil	0.9	12190	-0.386	1.082	-0.451	1.654	2.064
Max AB	0.9	12190	-0.419	1.225	0.086	0.423	1.365
Mil	1.4	12190	-0.227	0.664	-0.238	0.907	1.171
Max AB	1.4	12190	-0.249	0.724	0.060	0.214	0.797
Mil	0.9	15240	-0.654	1.788	-0.723	2.455	3.190
Max AB	0.9	15240	-0.718	2.123	0.152	0.593	2.323

* Pressure measurement errors and ranges are shown in Table 6.

Note: Sensitivity calculated for calibration #1, standard mode data.

Table 7. Effect of pressure measurement errors on HiMAT thrust algorithm computed thrust
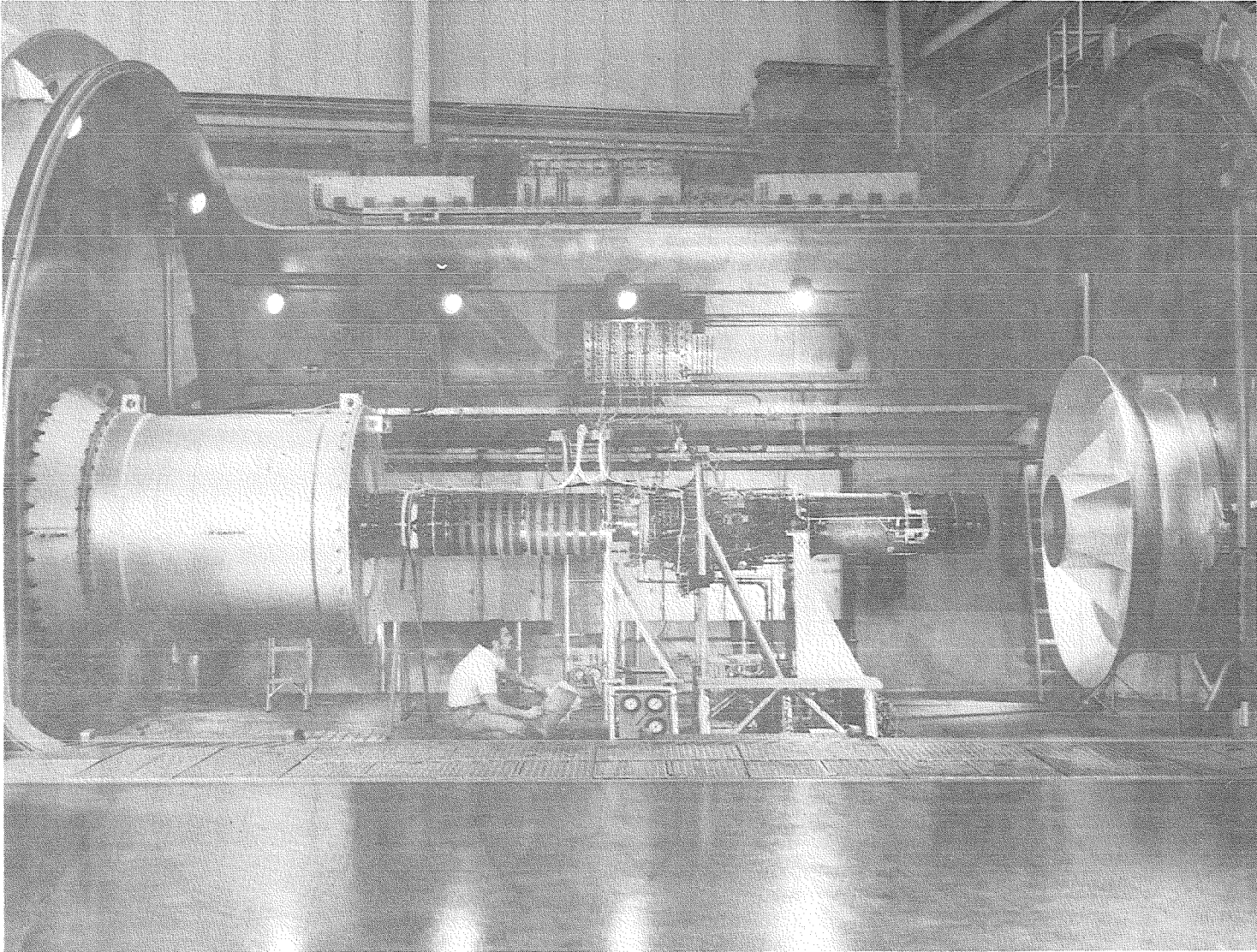
Figure 1. J85-GE-21 engine installed in altitude facility

(a) Station locations

Total pressure ○
Static pressure □
Temperature ✕
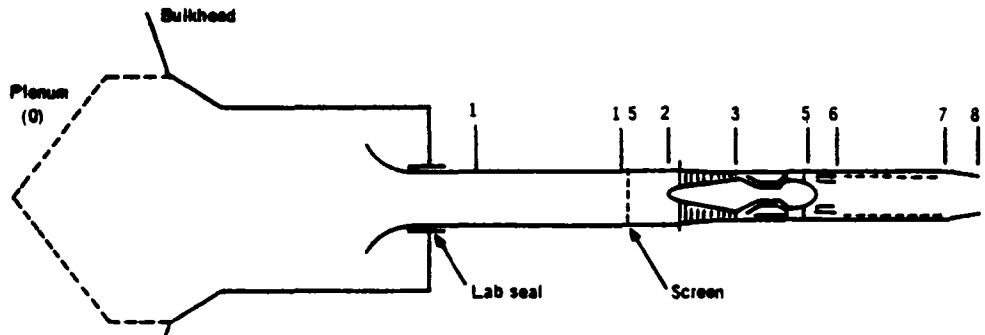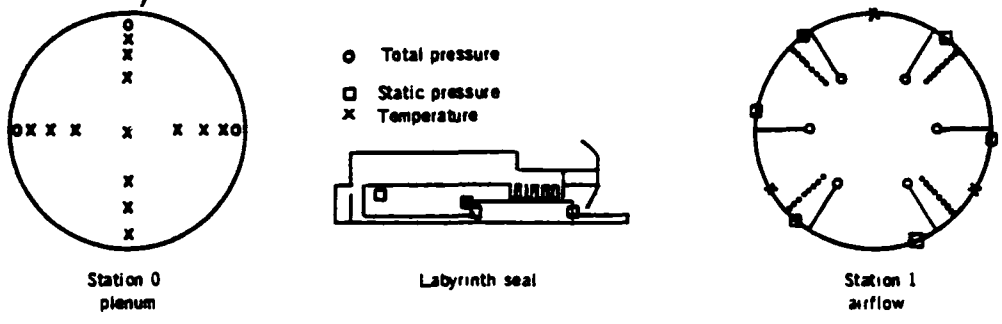
Station 0
plenum

Labyrinth seal

Station 1
airflow
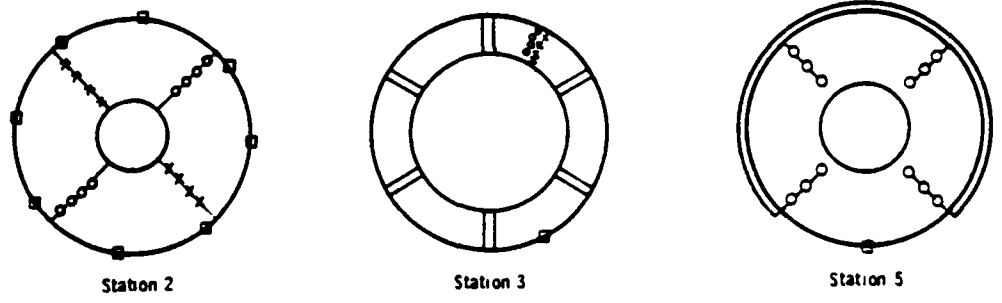
Station 2

Station 3

Station 5
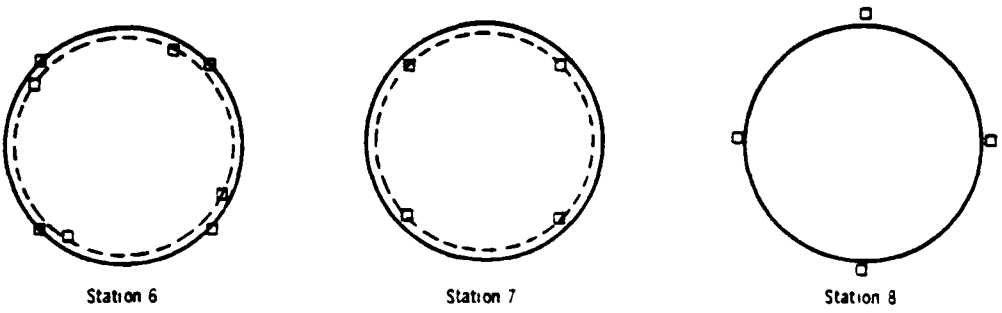
Station 6

Station 7

Station 8

b) Individual stations

Figure 2. Engine instrumentation
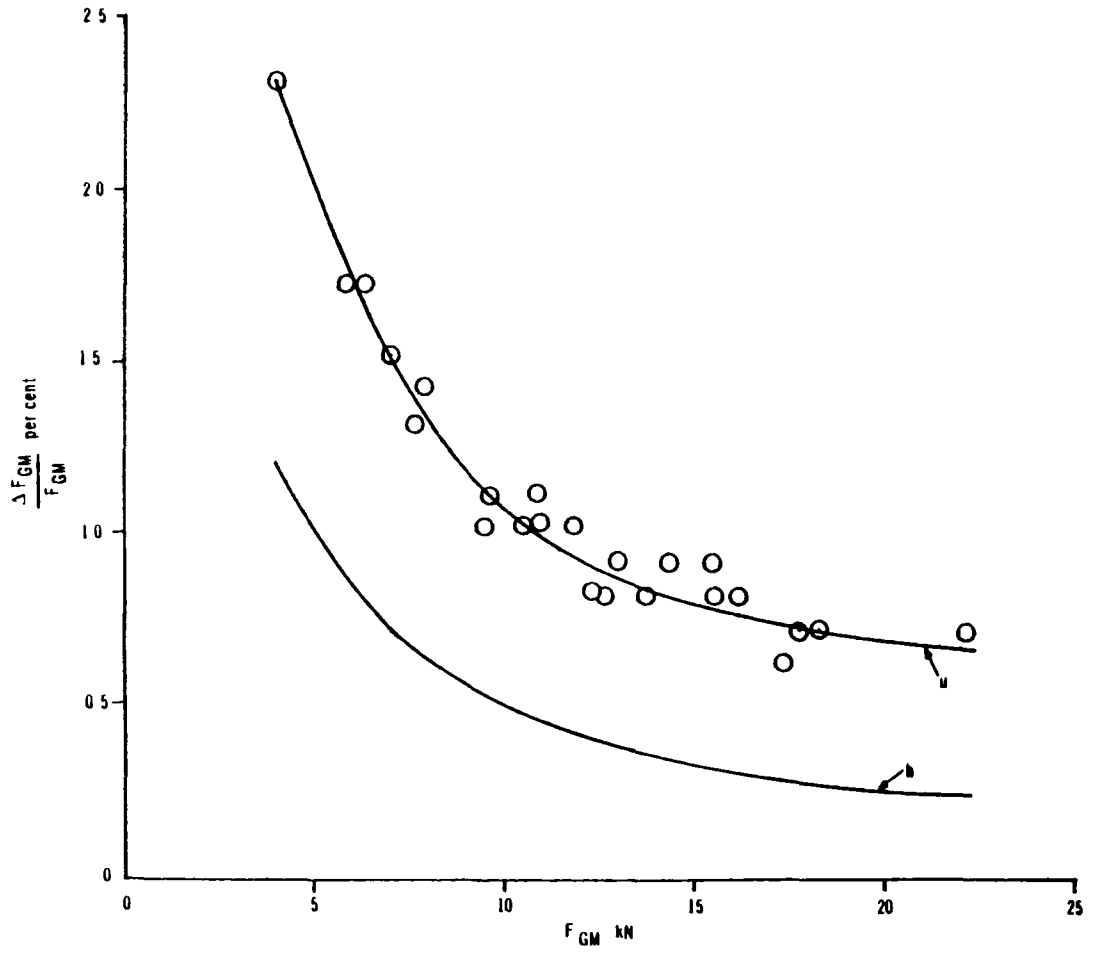
Figure 3   NASA Lewis facility gross thrust bias limit and total uncertainty

Engine stations

Engine pressure probes

P_{T5} — Turbine discharge total pressure

P_{S6} — Flameholder static pressure

P_{S7} — Nozzle entry static pressure

P_{TS} P_{S6} P_{S7}

Outlet bracket
mounted on compressor
front frame
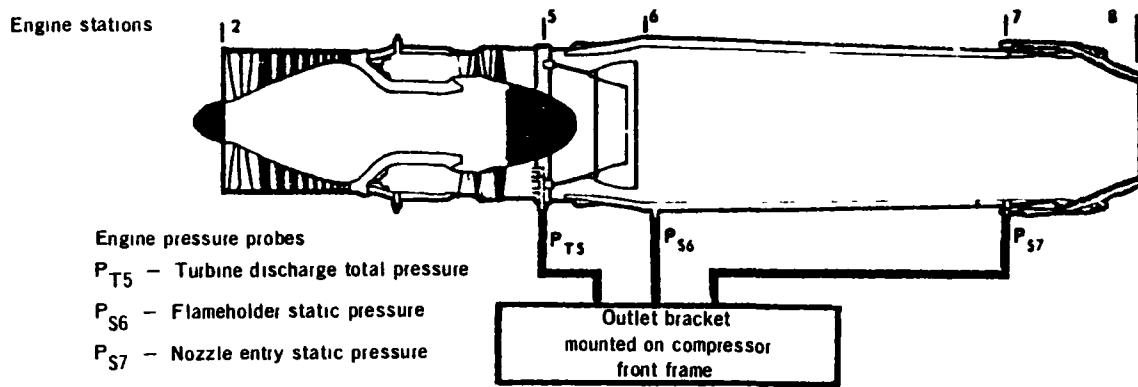
Figure 4   Tailpipe measurement stations
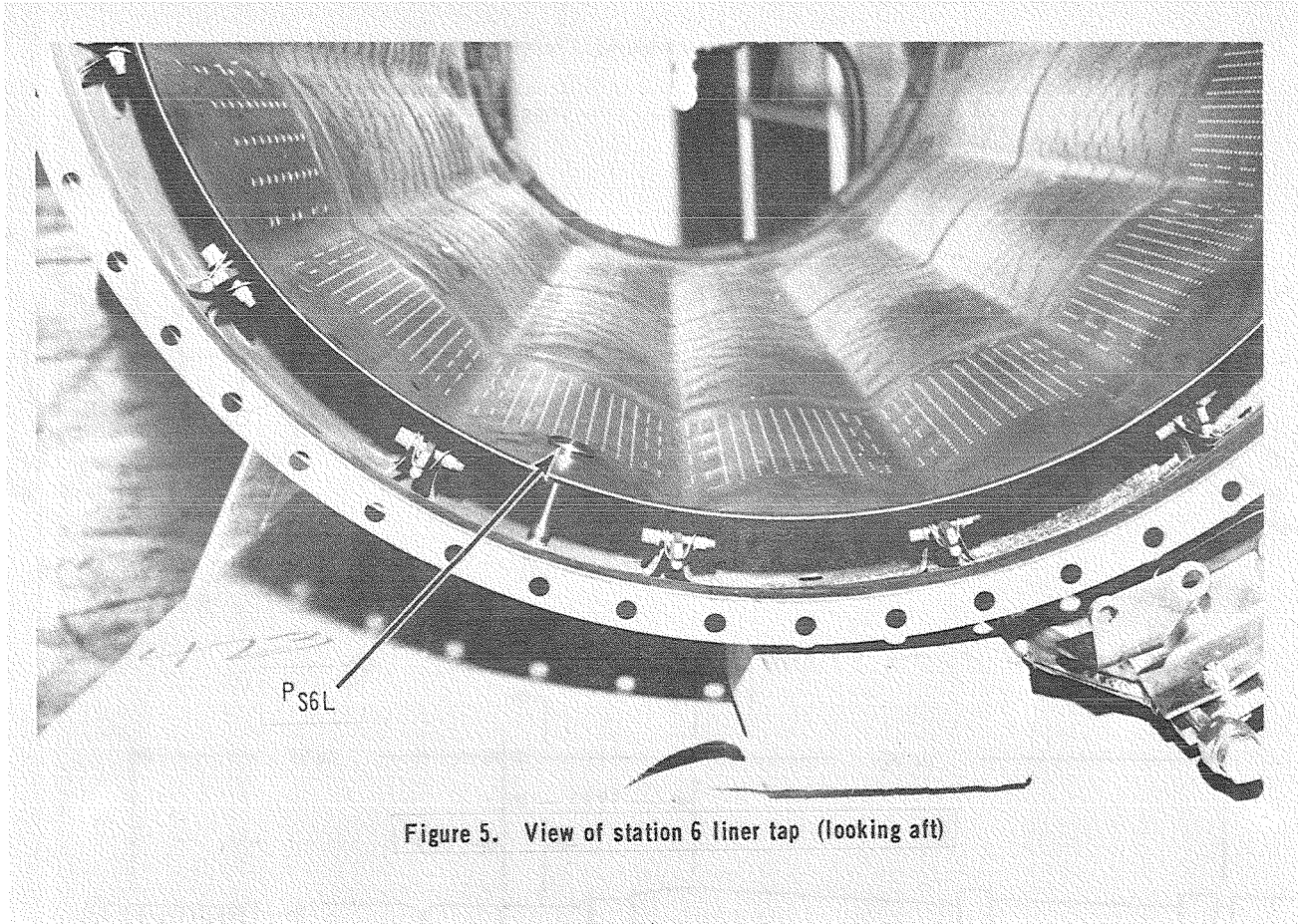
Figure 5. View of station 6 liner tap (looking aft)
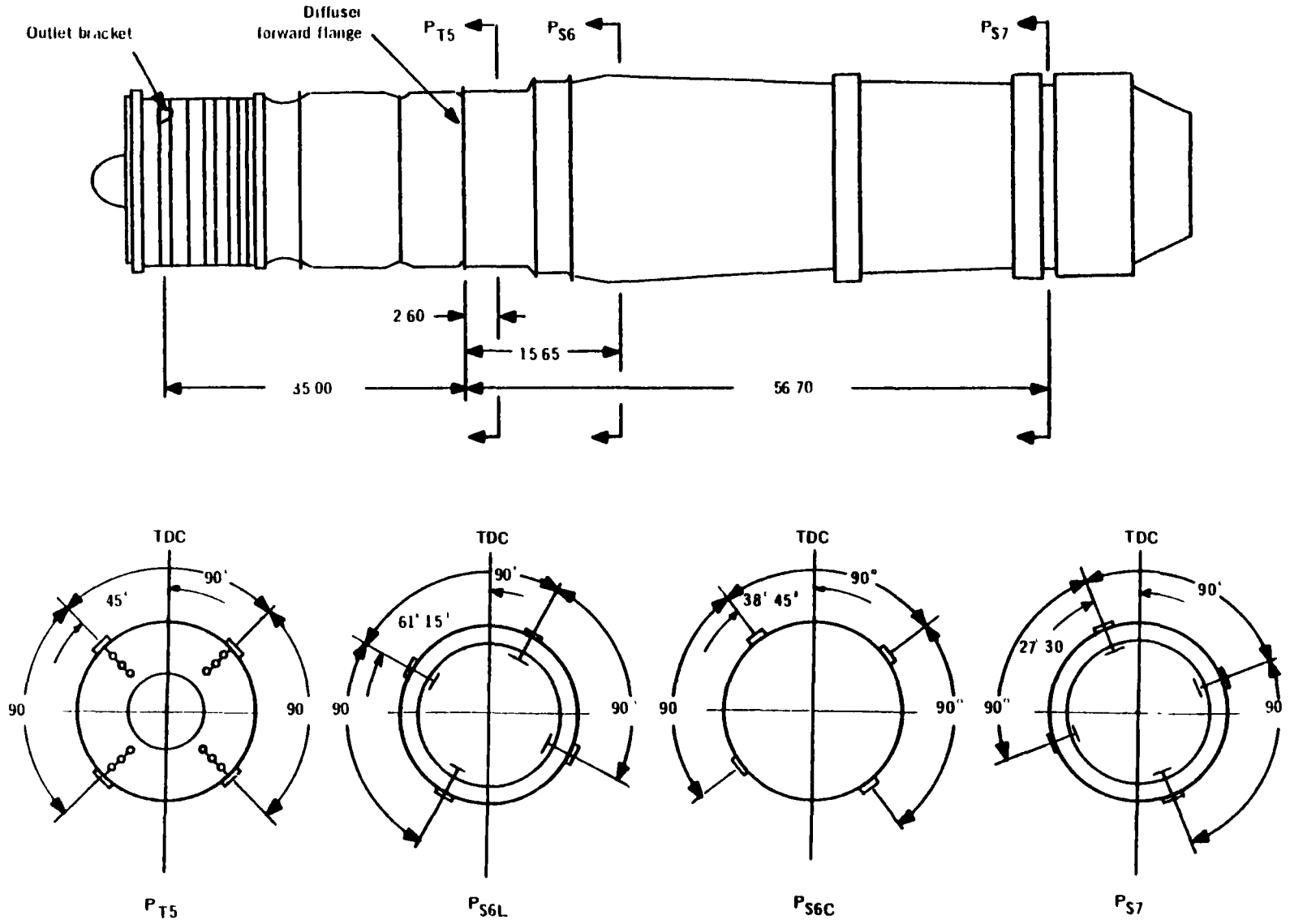
Figure 6   Tailpipe probe and manifold locations
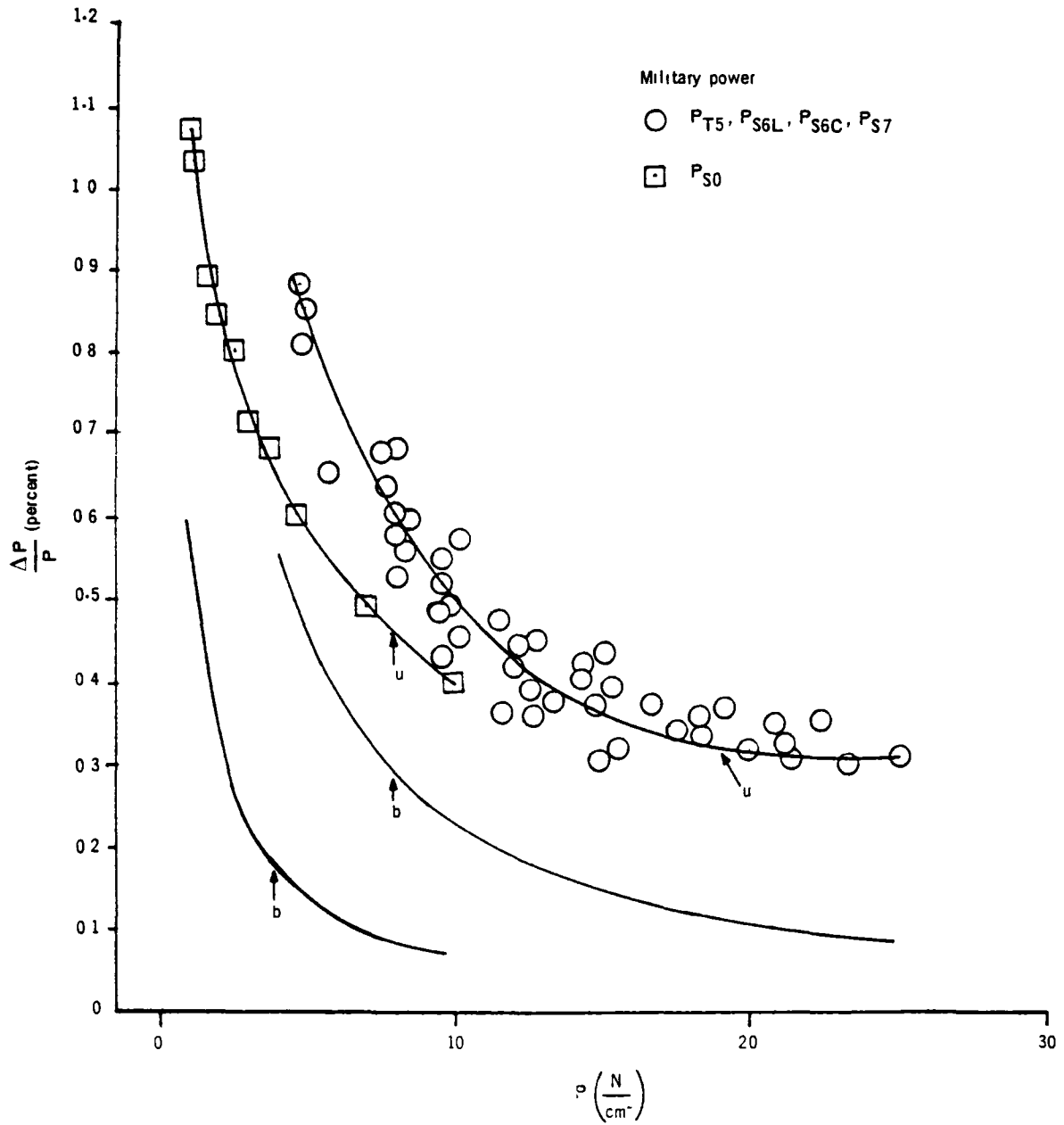
Figure 7.   NASA Lewis pressure transducer bias limit and total uncertainty

AO11/FR
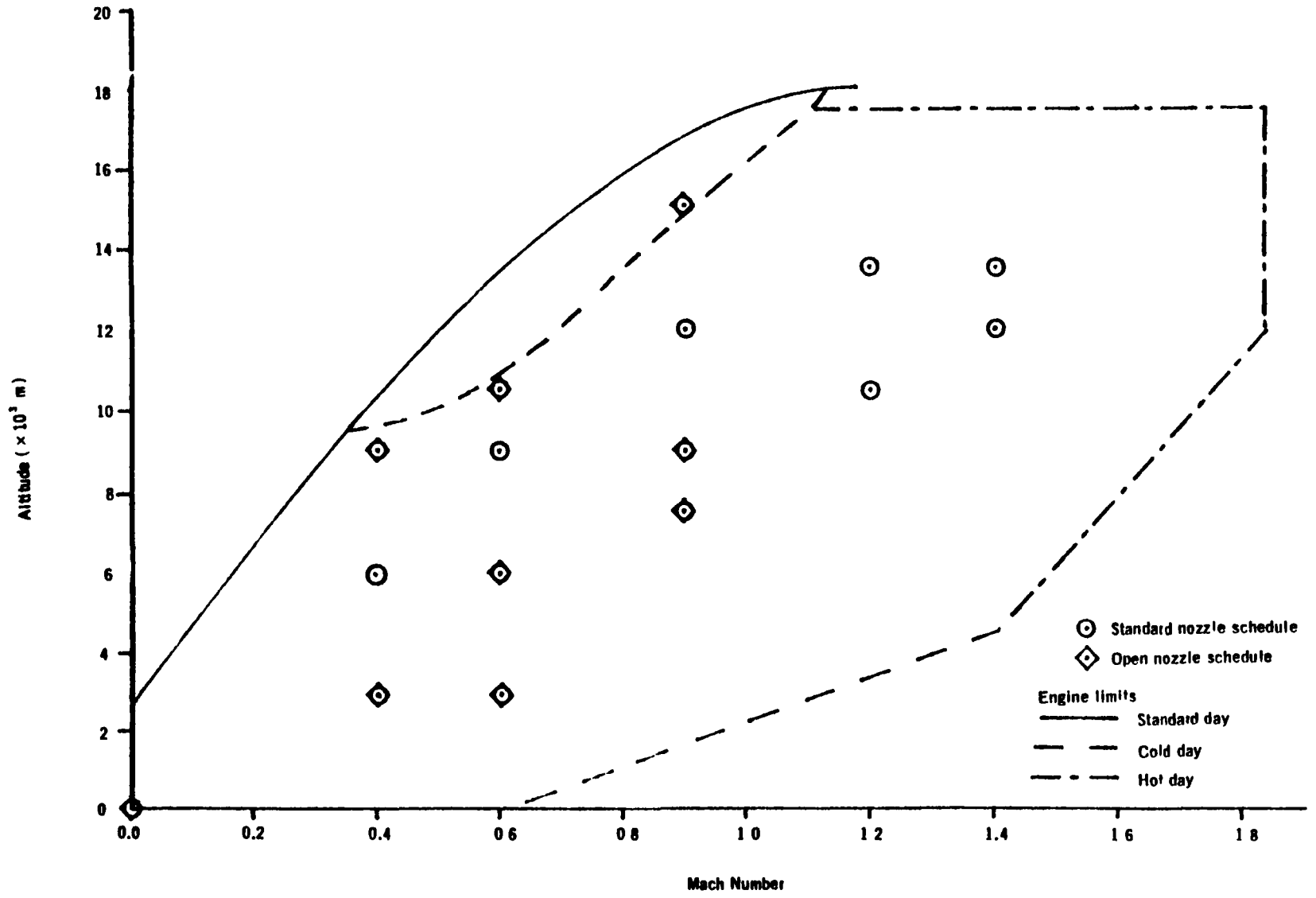
Figure 8.   Test Conditions
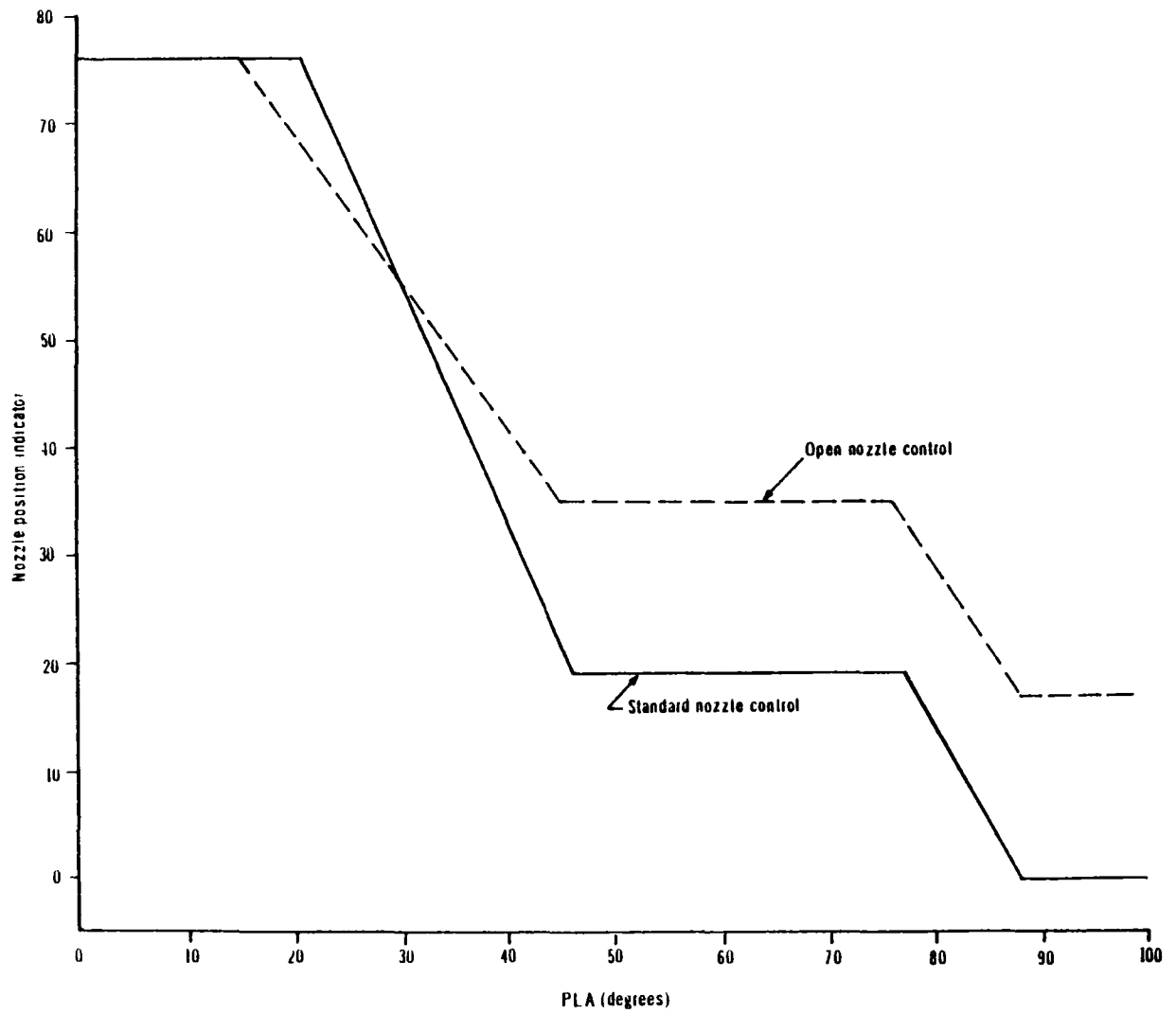
Figure 9   Standard and open nozzle schedules
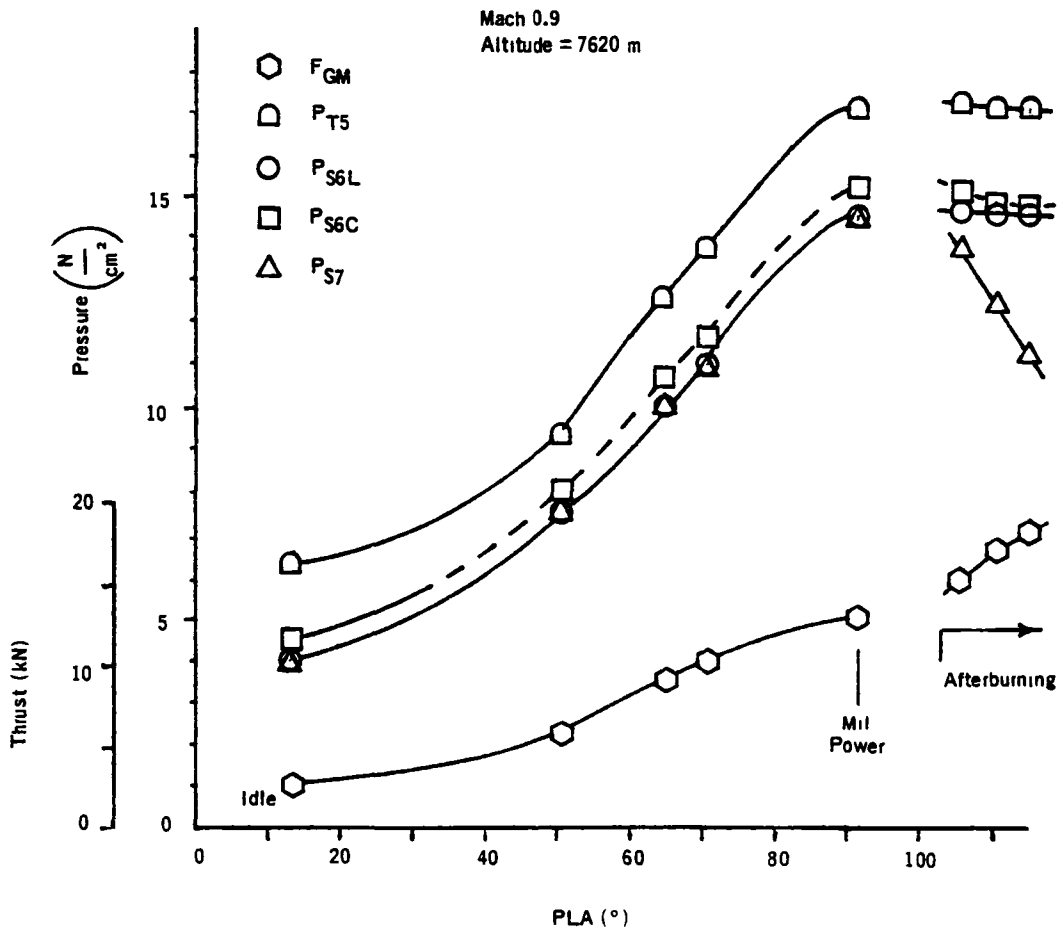
Figure 10.   Behaviour of tailpipe pressures
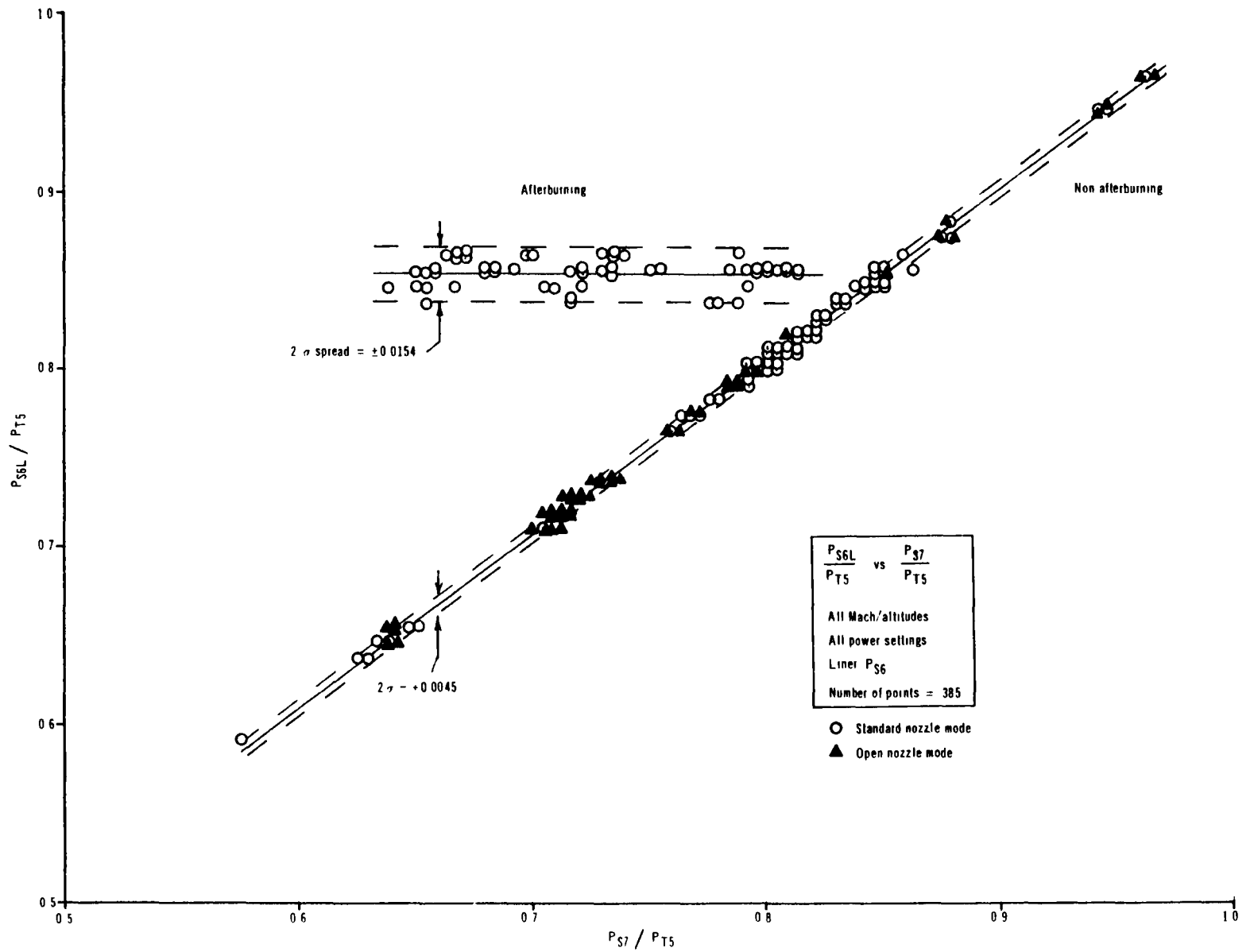
Figure 11   Tailpipe pressure diagnostics, liner P_{S6}
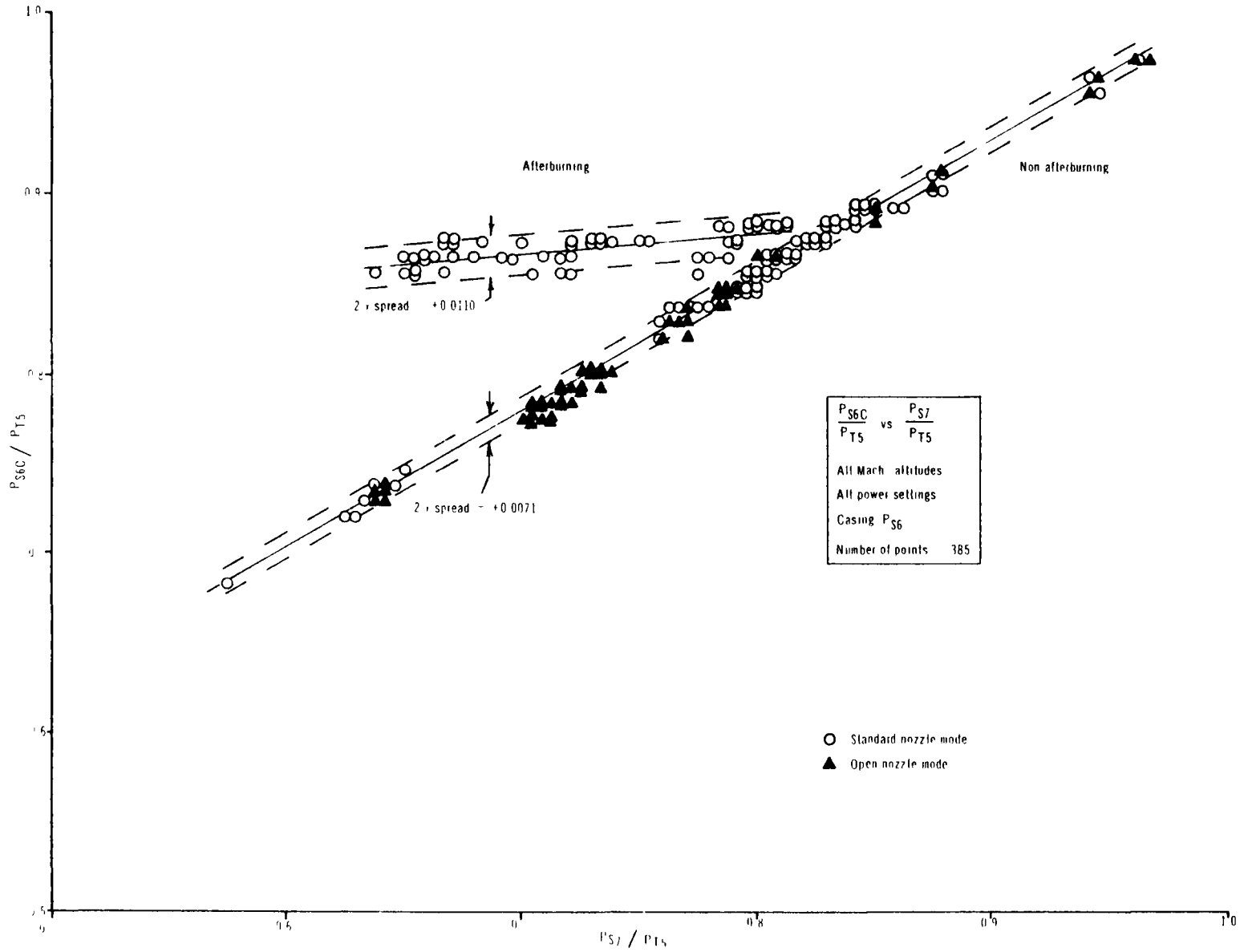
Figure 12   Tailpipe pressure diagnostics casing P_{S6}
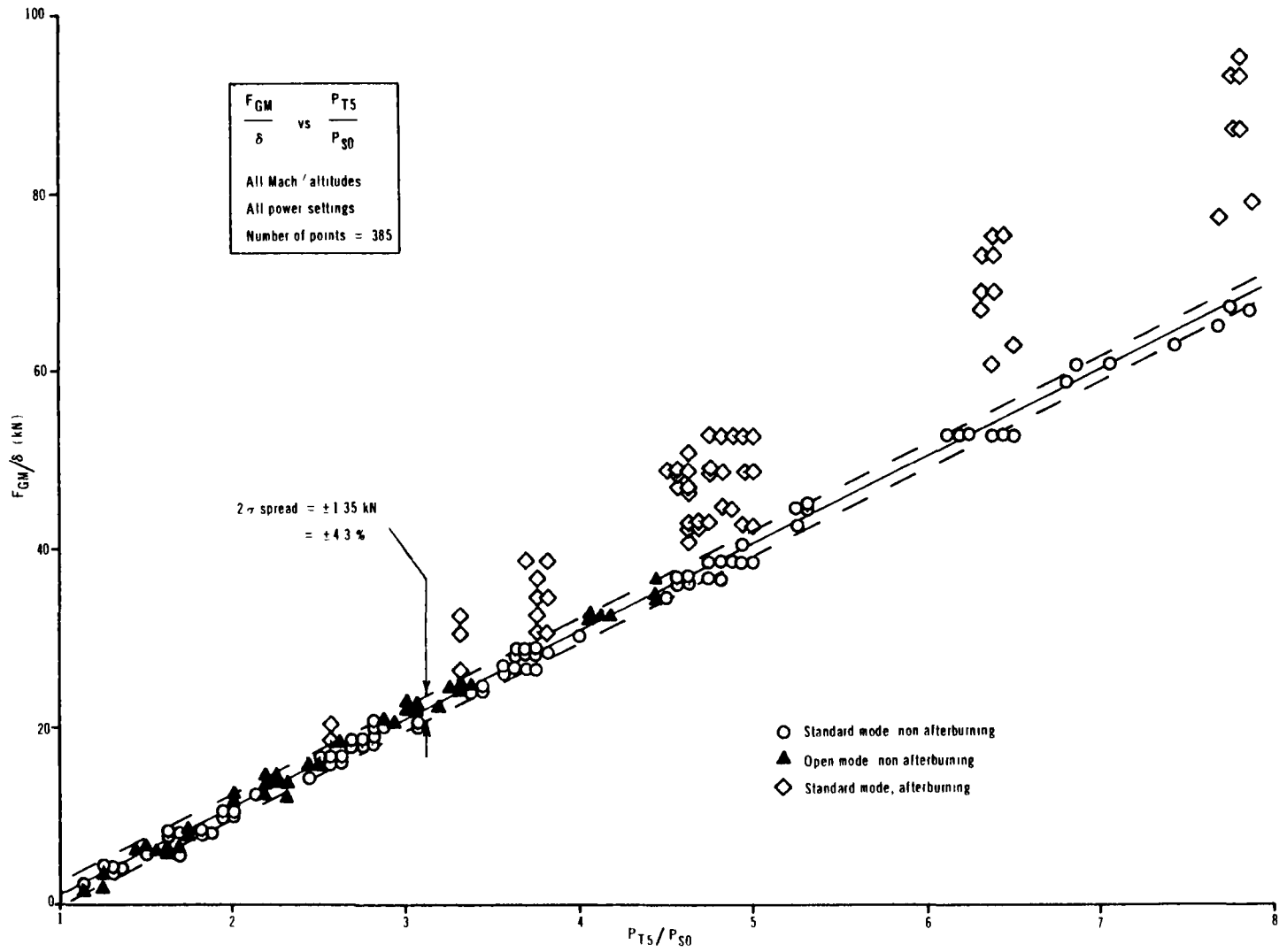
Figure 13 Thrust versus pressure diagnostic
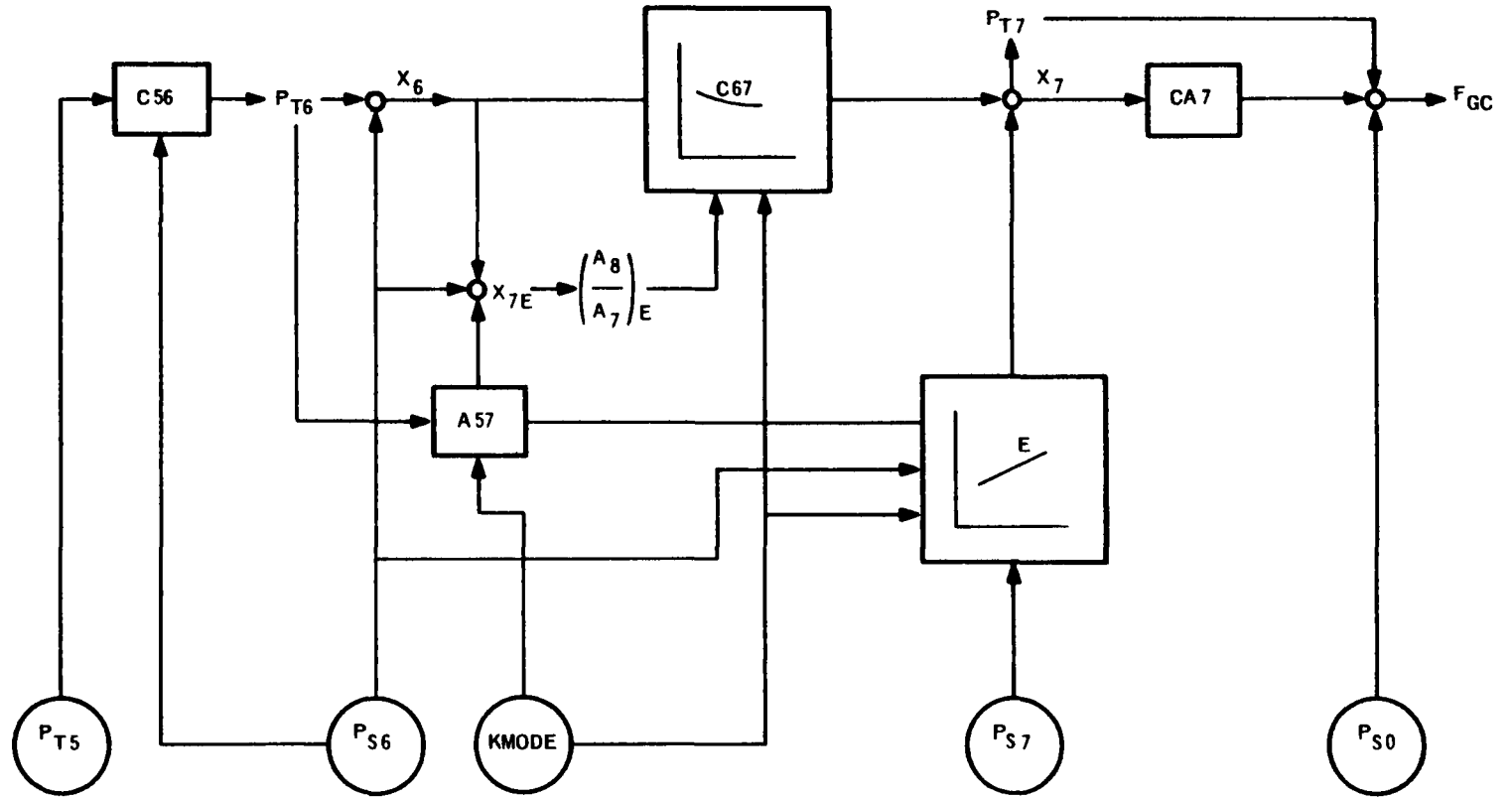
Figure 14   Schematic representation of thrust algorithm
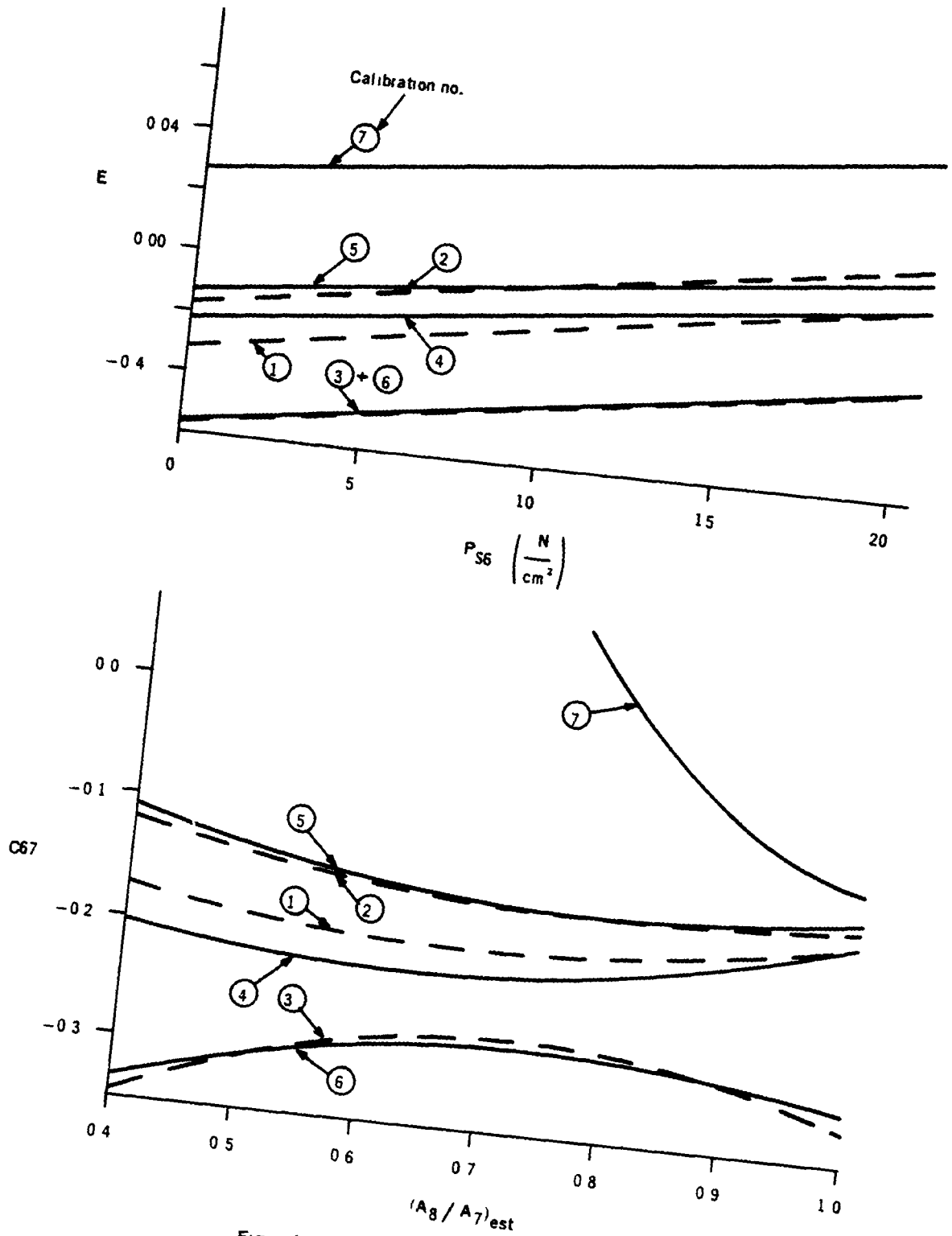
Figure 15   Variable calibration coefficients, E and C67
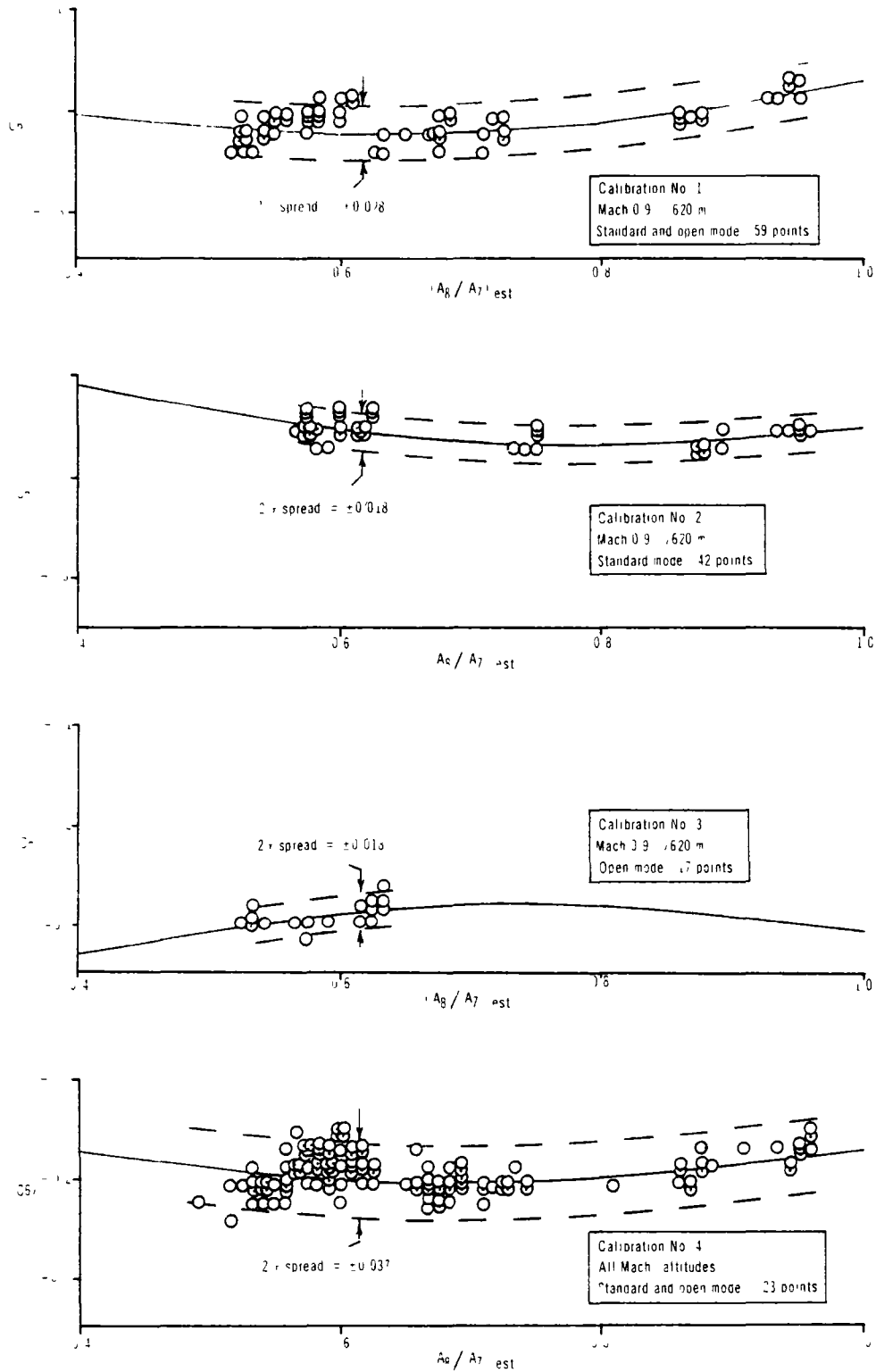
Figure 16 Scatter in calibration coefficient C67 (page 1 of 2)

Figure 16 Scatter in calibration coefficient C67 (page 2 of 2)

$$\left(\frac{F_{GC} - F_{GM}}{F_{GM}}\right) \times 100 \quad \text{vs} \quad F_{GM}$$

Thrust prediction using calibration No 1

Liner P_{S6} taps

Standard and open nozzle mode

All Mach / altitude test conditions

Non repeat points used

Number of points = 128

Bias 0 16%

2 / spread = ±2 27%
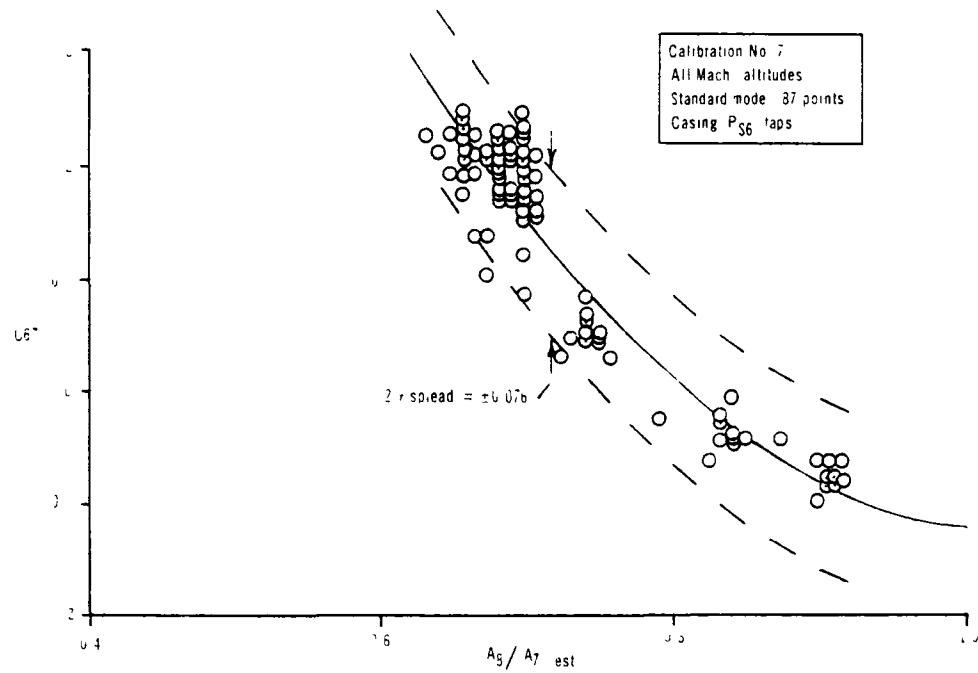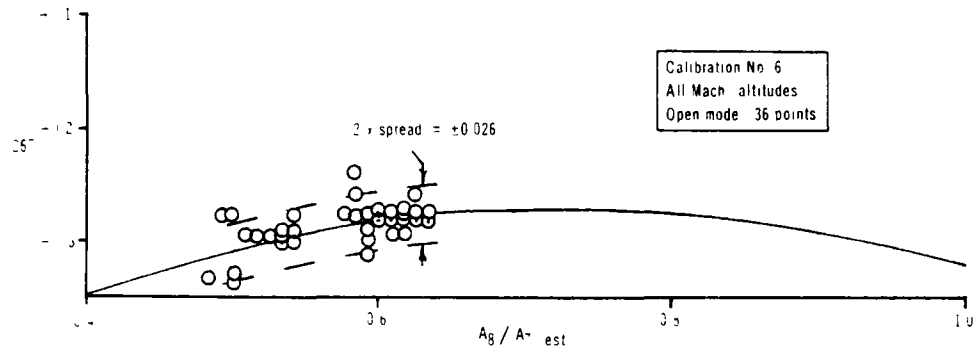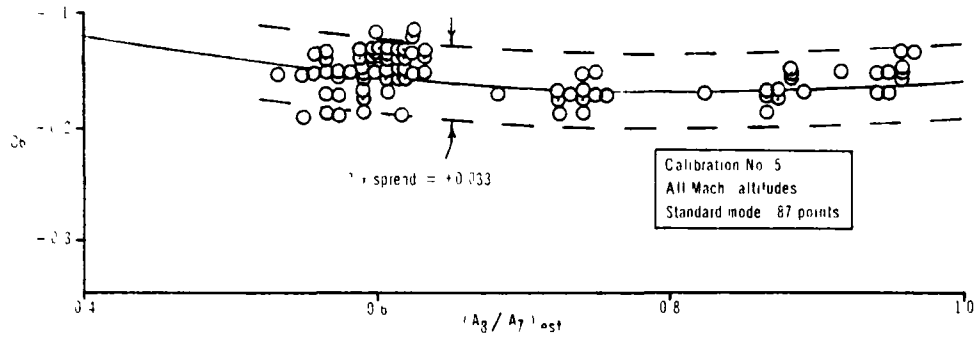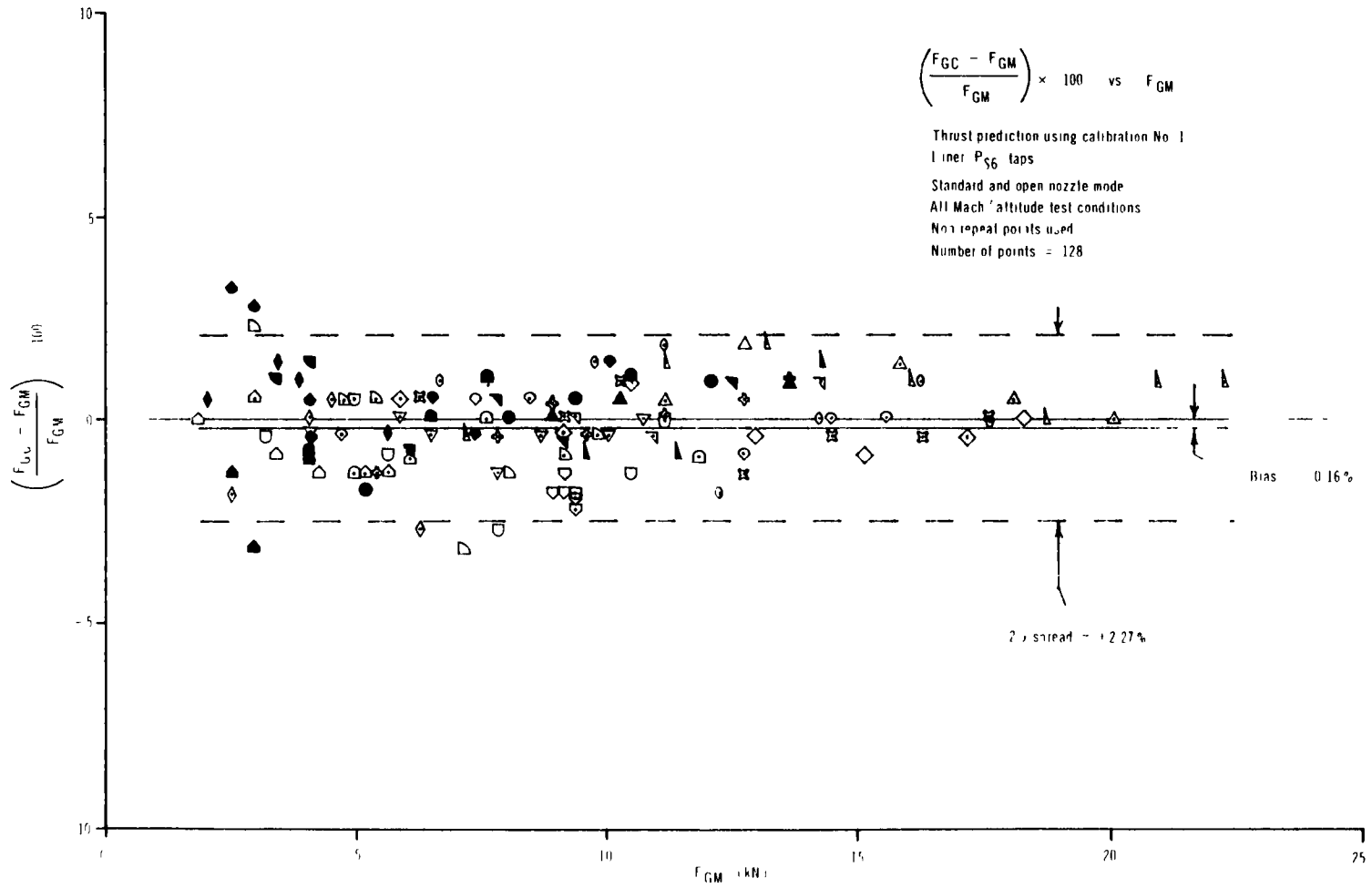
Figure 17   Thrust prediction on standard and open mode data using calibration No 1
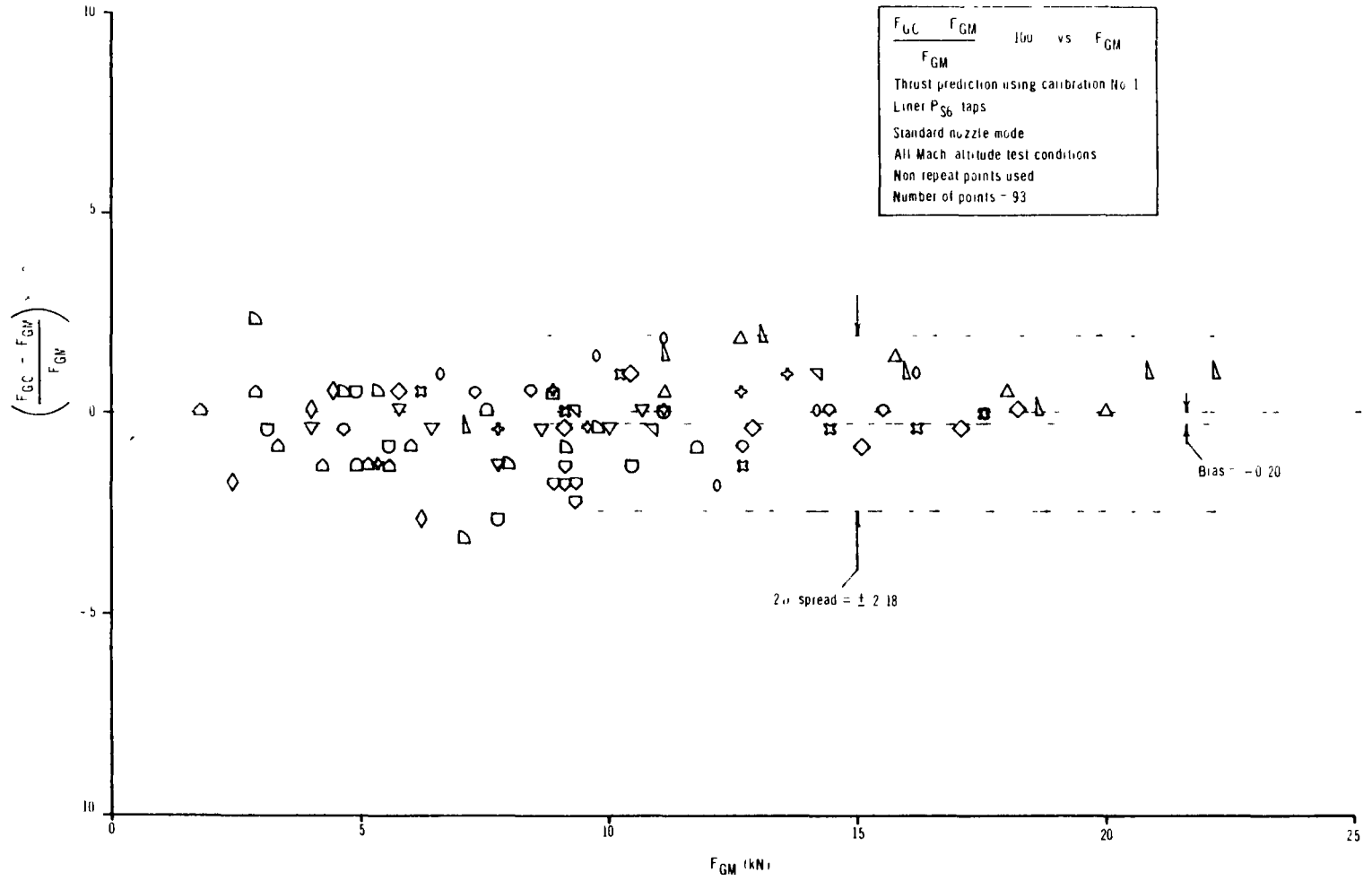
Figure 18   Thrust prediction on standard mode data using calibration No 1
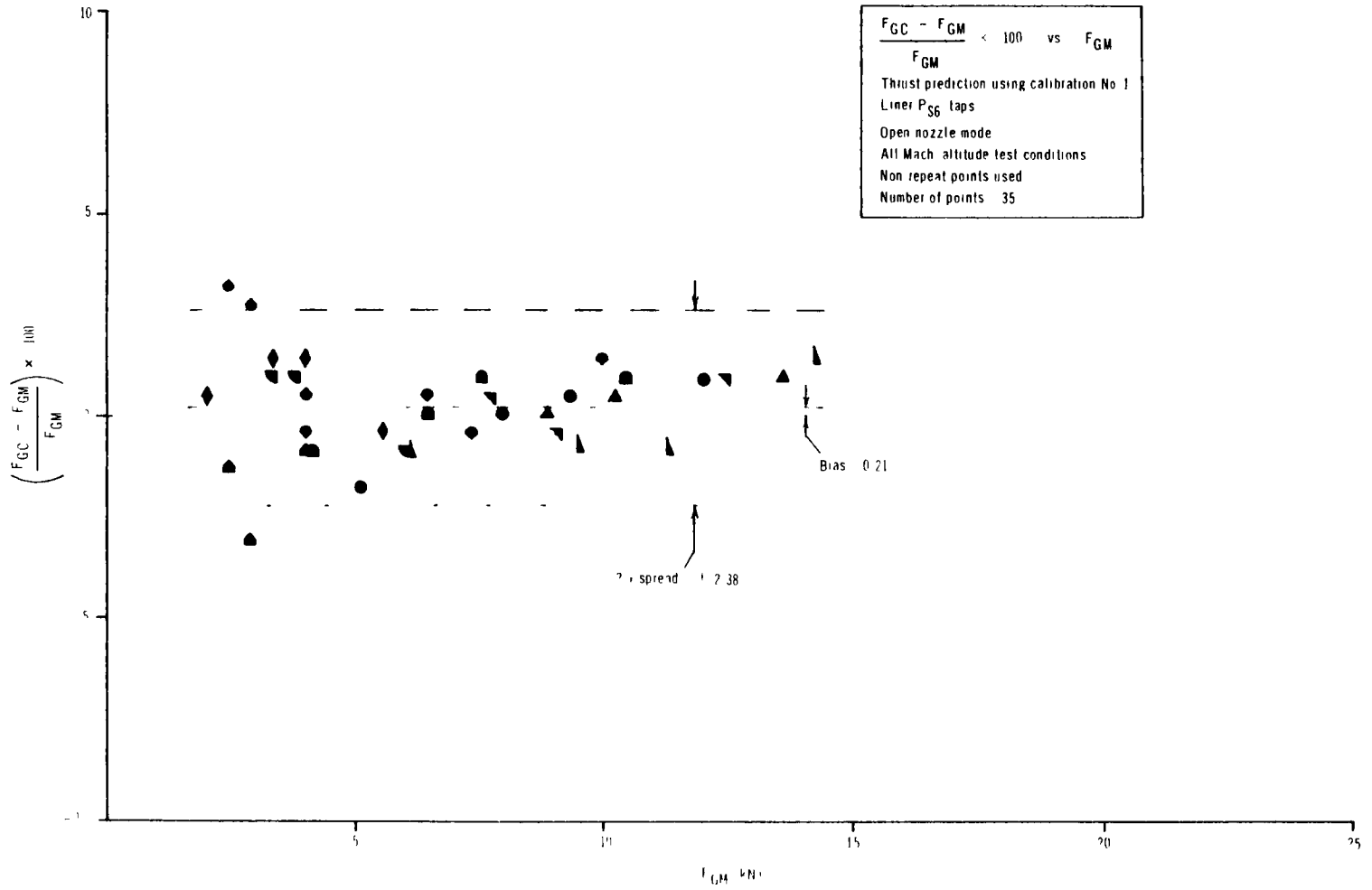
Figure 19   Thrust prediction on open mode data using calibration No 1
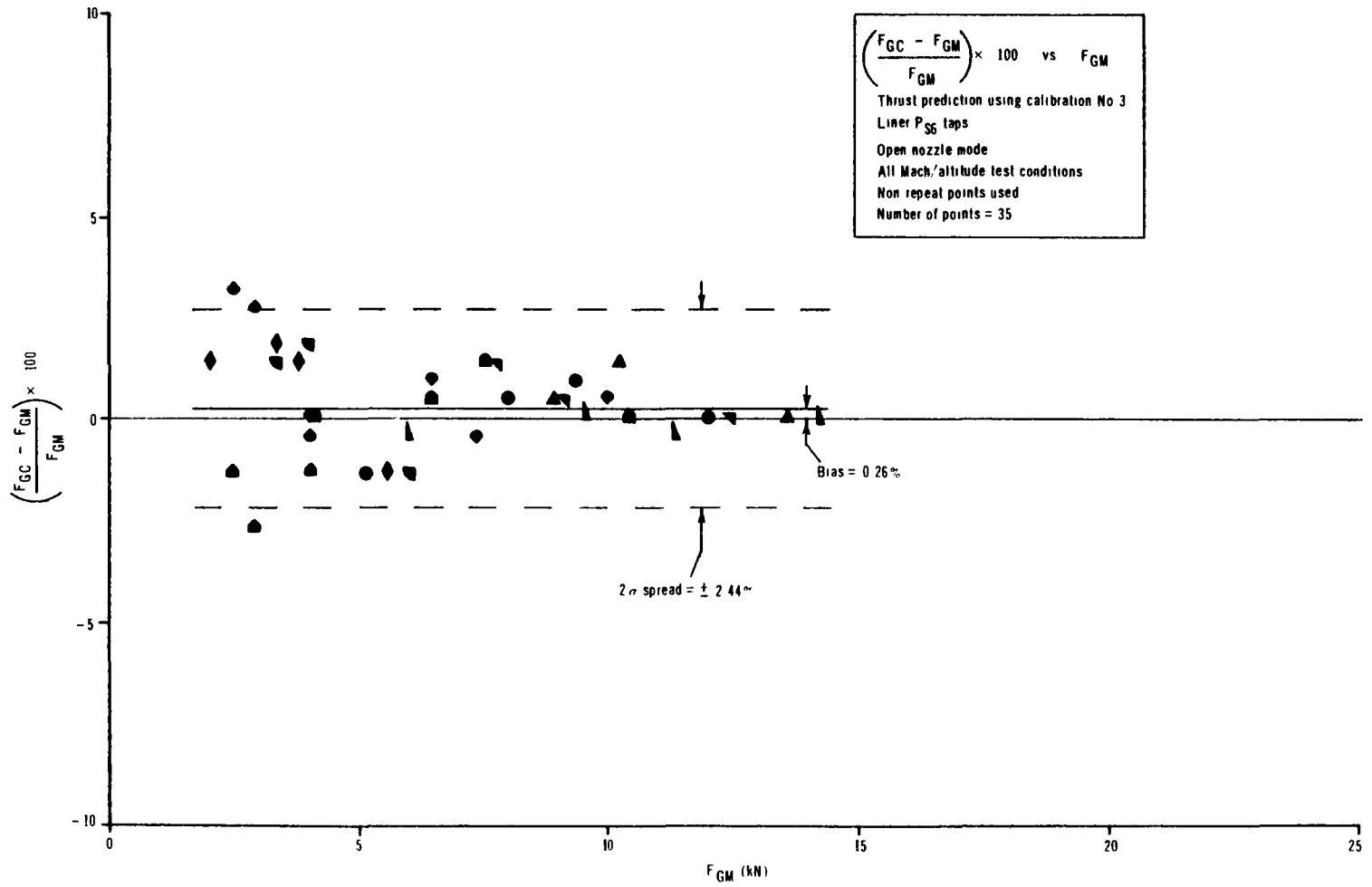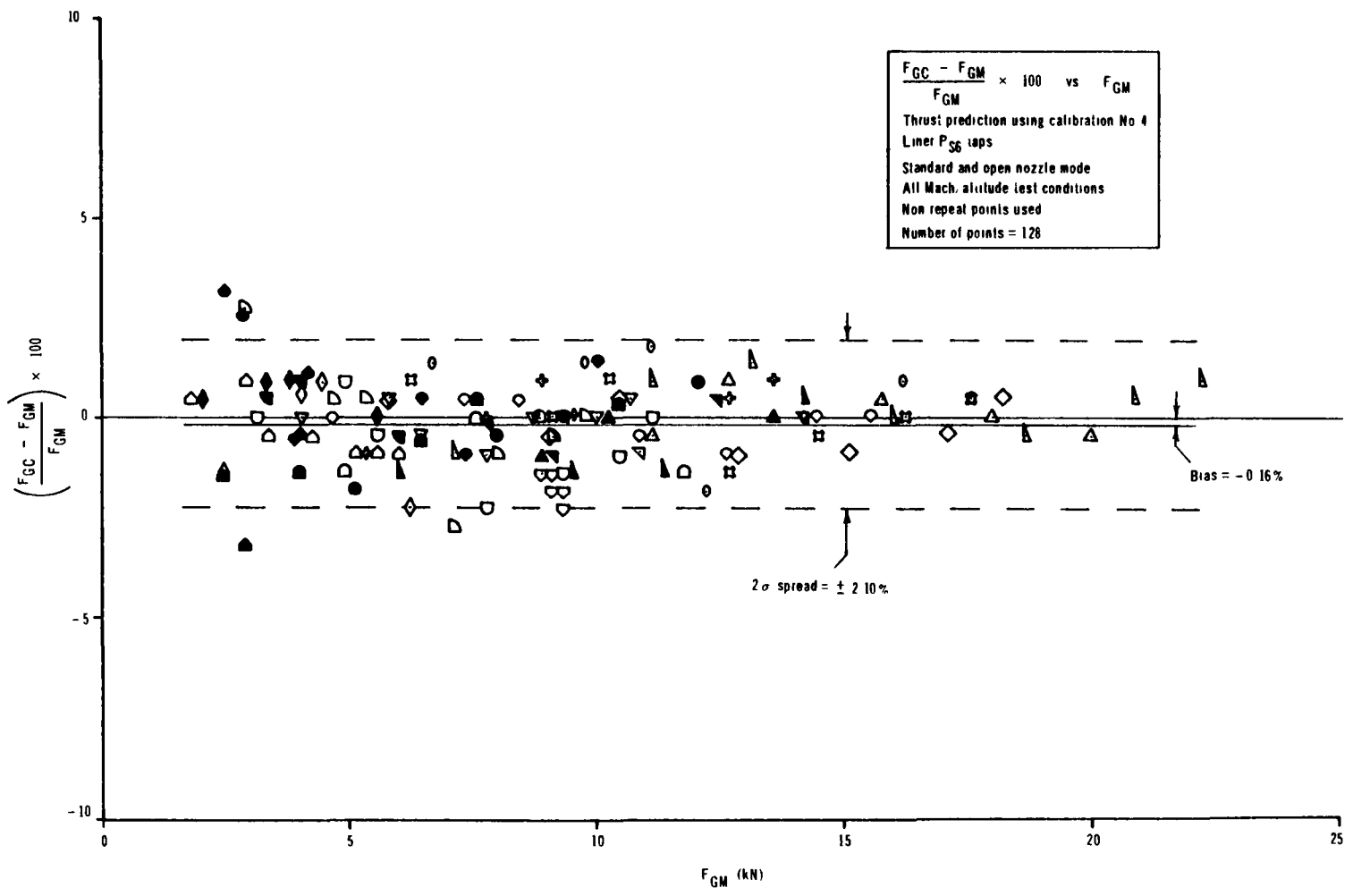
$$\frac{F_{GC} - F_{GM}}{F_{GM}} \times 100 \quad \text{vs} \quad F_{GM}$$

Thrust prediction using calibration No 2
Liner P_{S6} taps

Standard nozzle mode
All Mach/altitude test conditions
Non repeat points used
Number of points = 93

$\frac{F_{GC} - F_{GM}}{F_{GM}} \times 100$

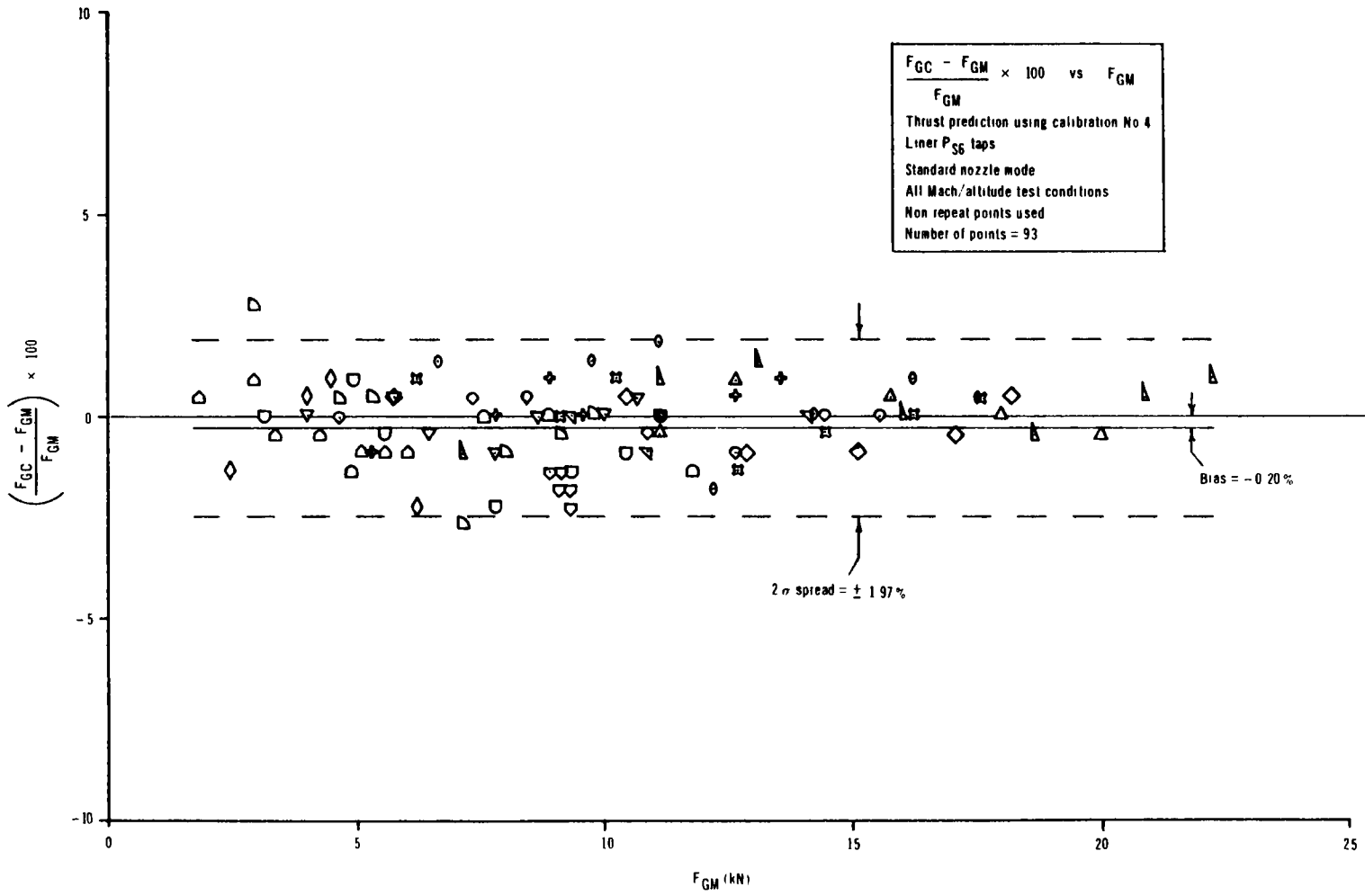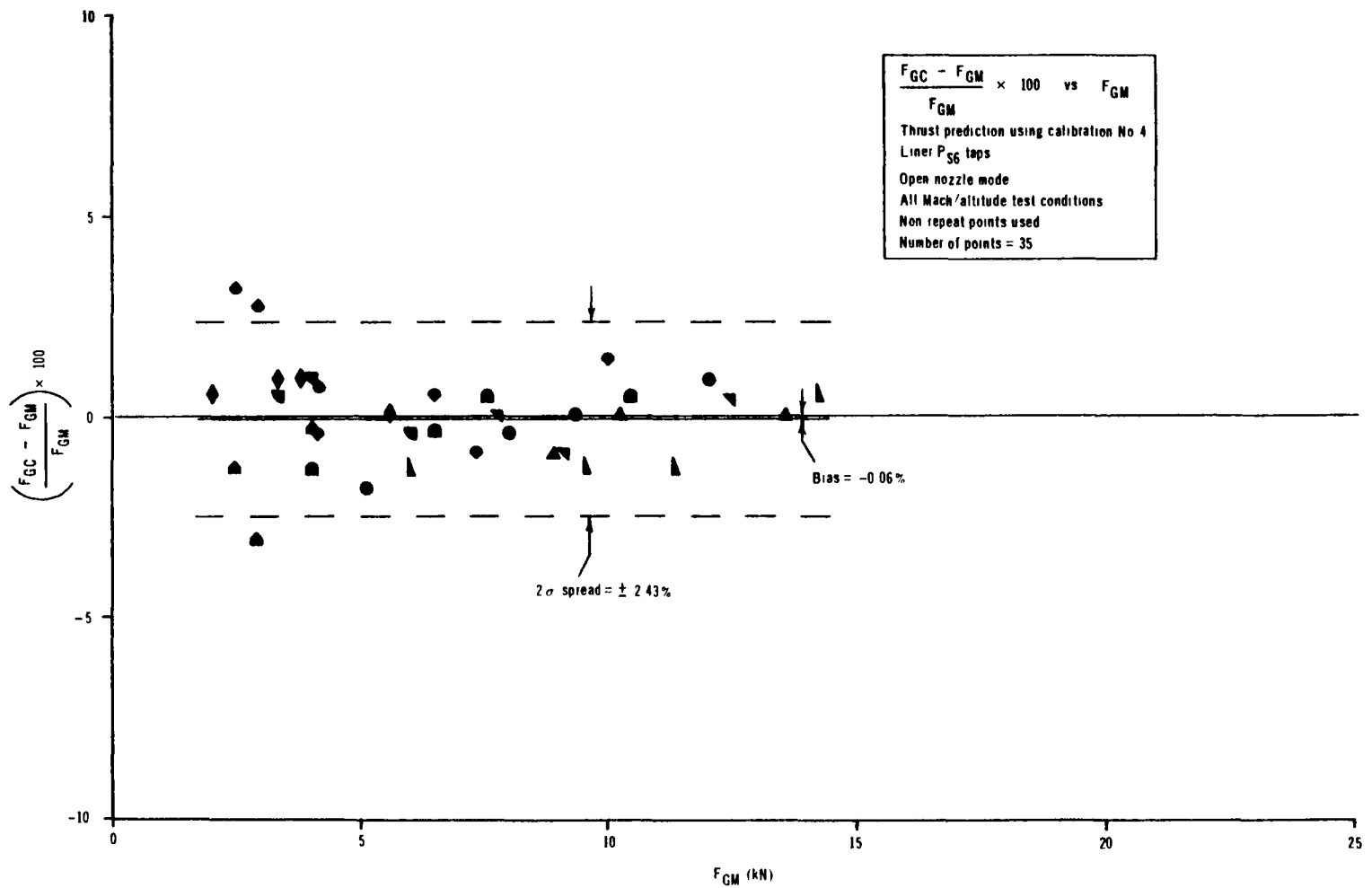Bias = –0 31%

2σ spread = ± 1 83%

F_{GM} (kN)
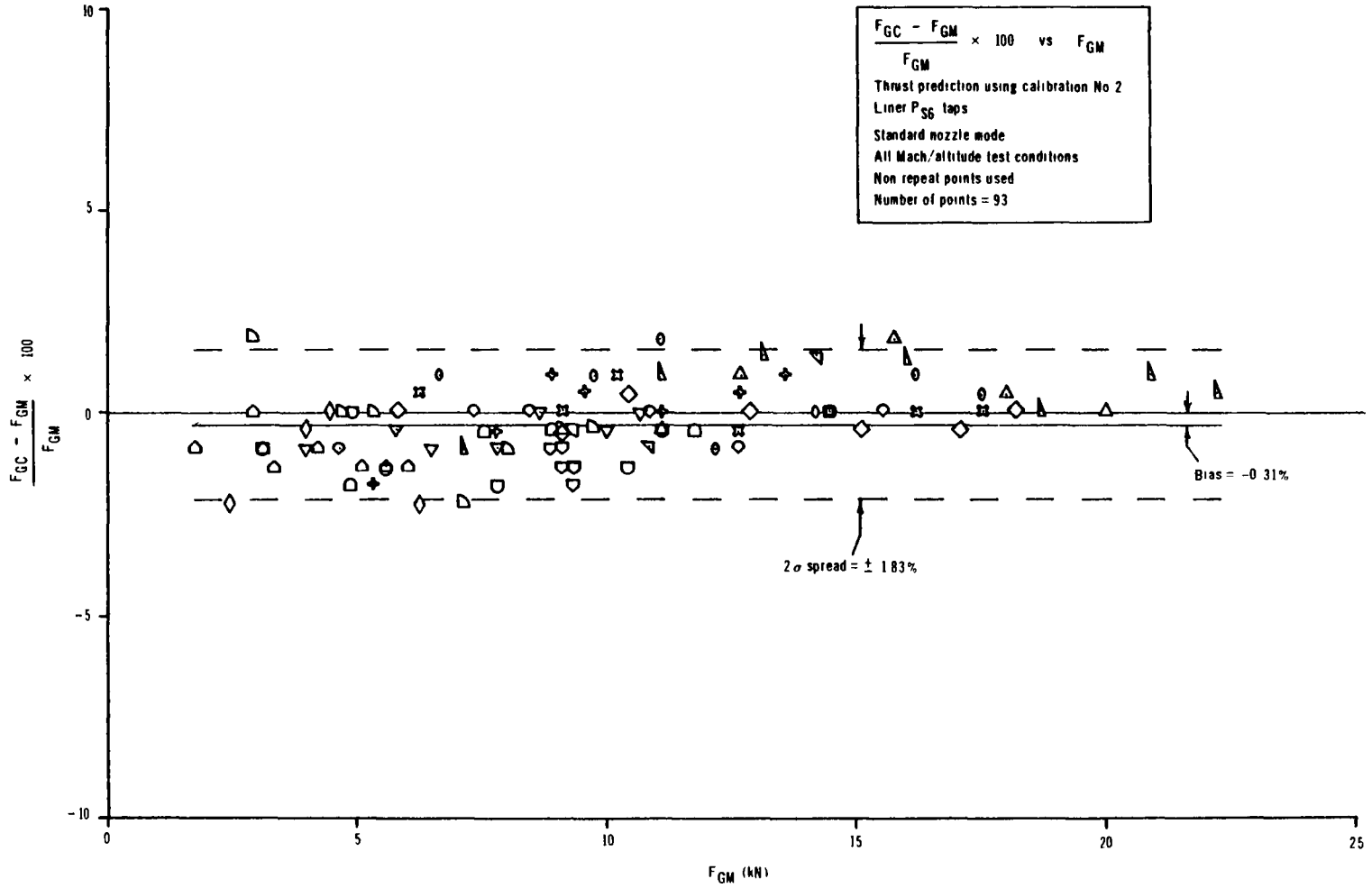
Figure 28   Thrust prediction on standard mode data using calibration No 2

Figure 21   Thrust prediction on open mode data using calibration No 3
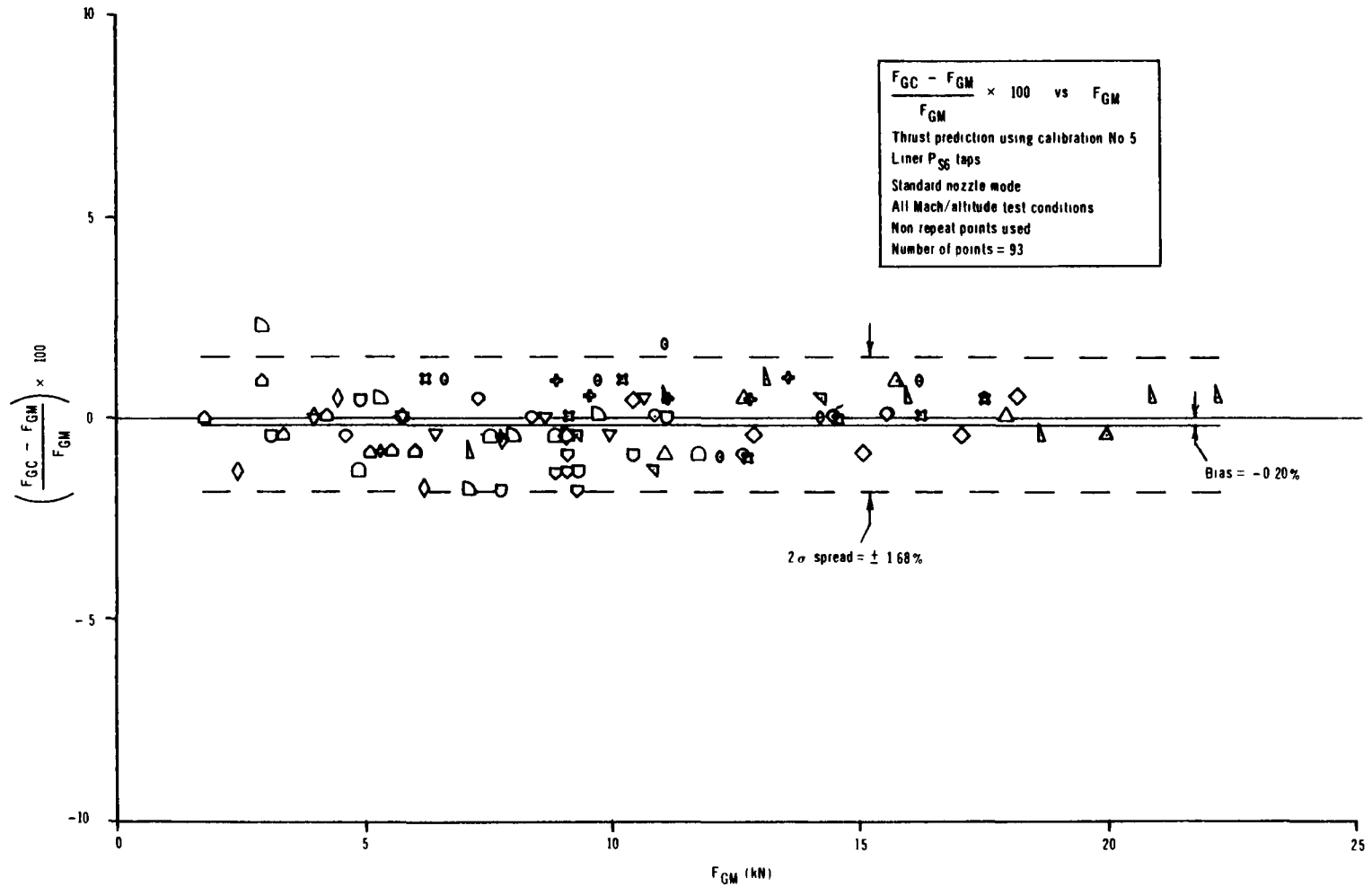
$$\left(\frac{F_{GC} - F_{GM}}{F_{GM}}\right) \times 100 \quad vs \quad F_{GM}$$

Thrust prediction using calibration No 4

Liner P_{S6} taps

Standard and open nozzle mode

All Mach, altitude test conditions

Non repeat points used

Number of points = 128

Bias = −0 16 %

2σ spread = ± 2 10 %

F_{GM} (kN)

Figure 22   Thrust prediction on standard and open mode data using calibration No 4

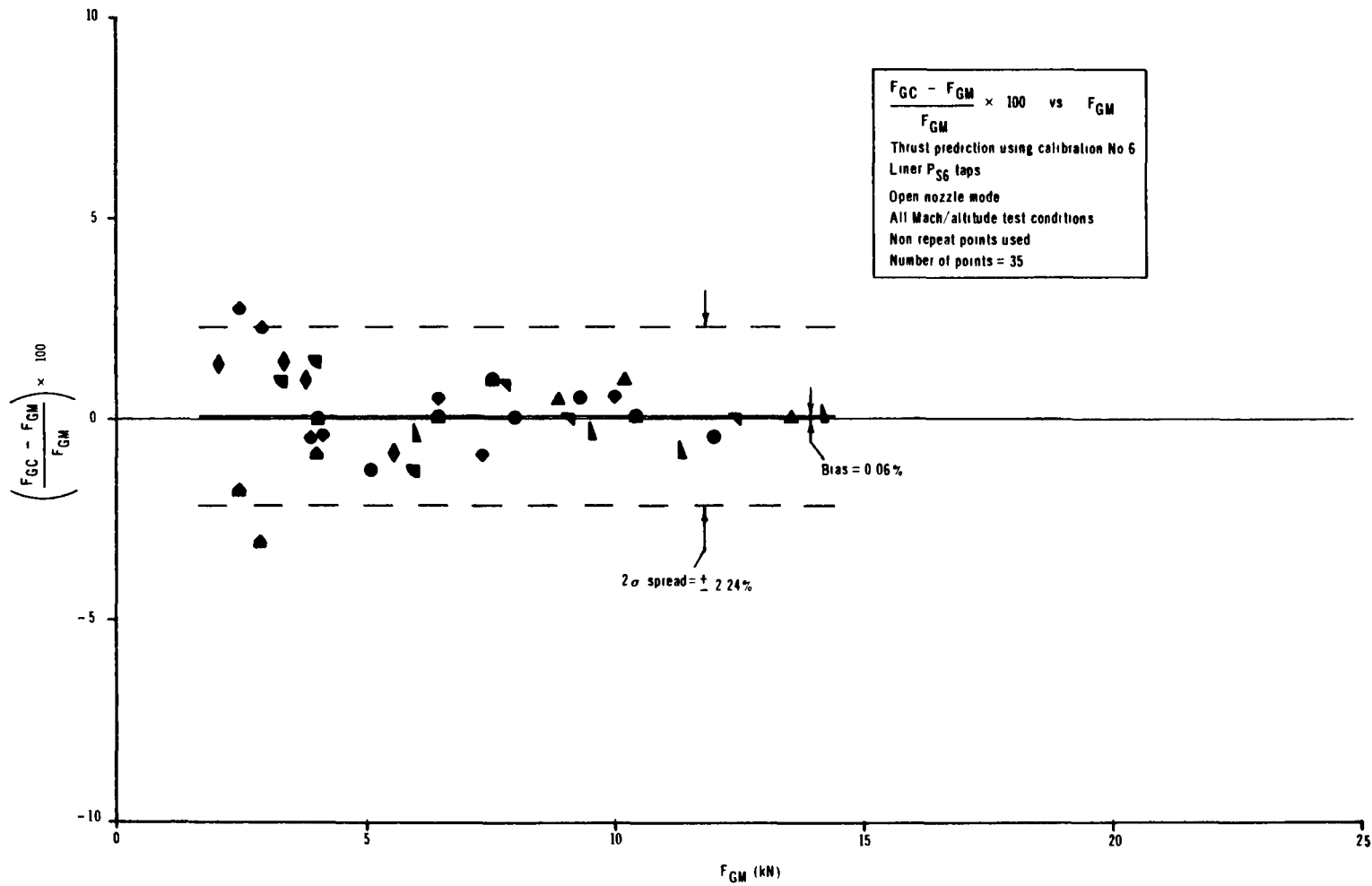Figure 23   Thrust prediction on standard mode data using calibration No 4

$$\frac{F_{GC} - F_{GM}}{F_{GM}} \times 100 \quad \text{vs} \quad F_{GM}$$

Thrust prediction using calibration No 4

Liner P_{S6} taps

Open nozzle mode

All Mach/altitude test conditions

Non repeat points used

Number of points = 35

Bias = -0 06 %

2σ spread = $\pm$ 2 43 %

Figure 24   Thrust prediction on open mode data using calibration No 4

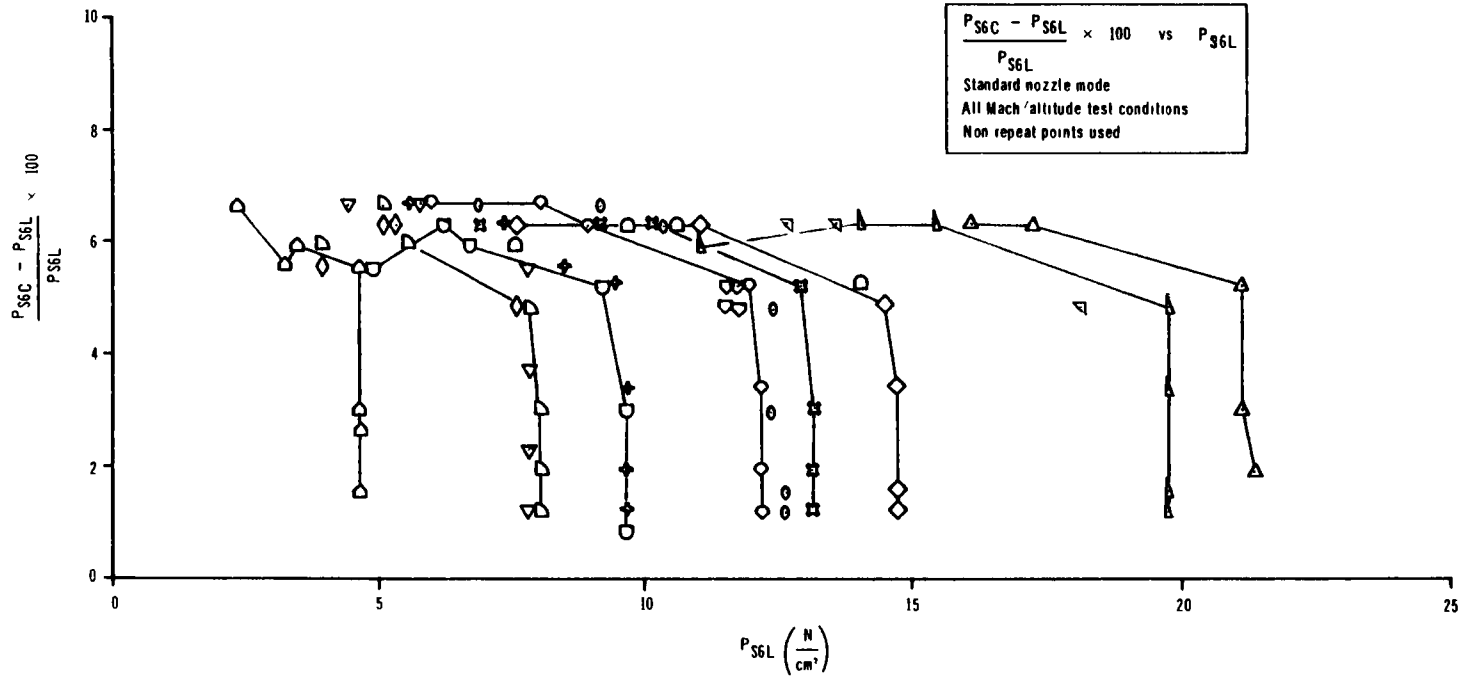Figure 25   Thrust prediction on standard mode data using calibration No 5

$$\frac{F_{GC} - F_{GM}}{F_{GM}} \times 100 \quad vs \quad F_{GM}$$

Thrust prediction using calibration No 6

Liner P_{S6} taps

Open nozzle mode

All Mach/altitude test conditions

Non repeat points used

Number of points = 35

Bias = 0 06 %

2σ spread= $\pm$ 2 24%

Figure 26   Thrust prediction on open mode data using calibration No 6

Figure 27   Comparison of casing with liner P_{S6} at each test condition, standard mode
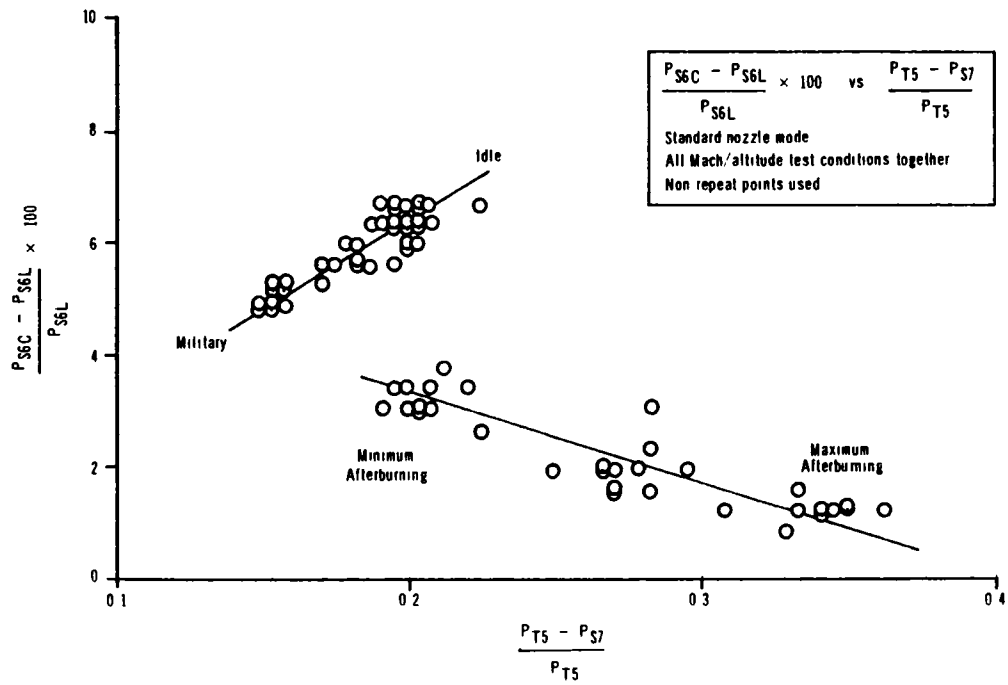
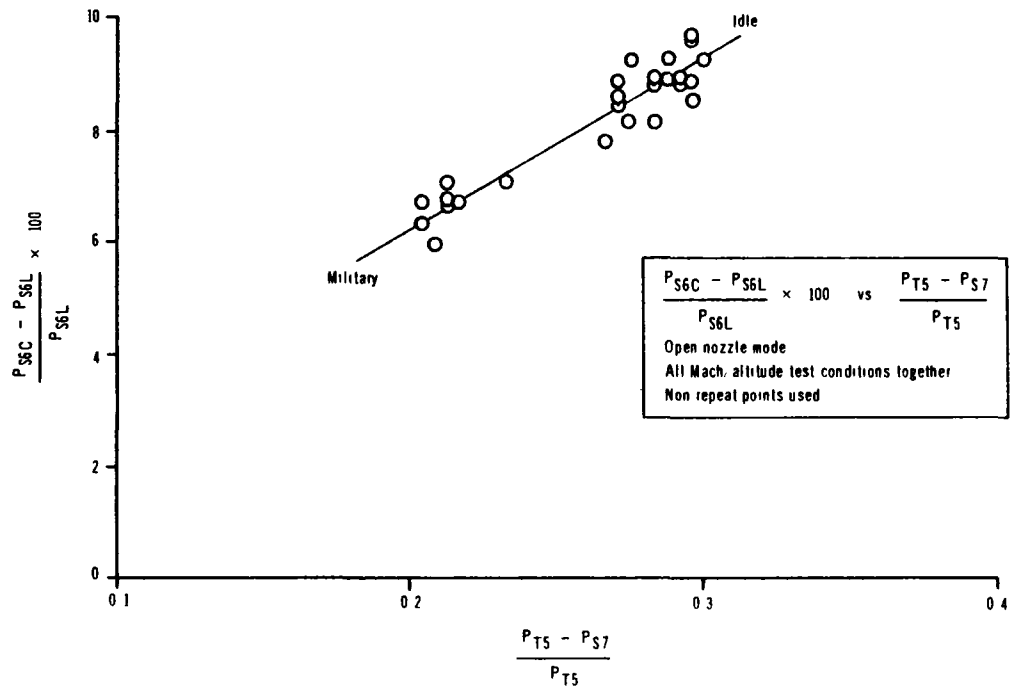Figure 28   Comparison of casing with liner P_{S6} normalized, standard mode

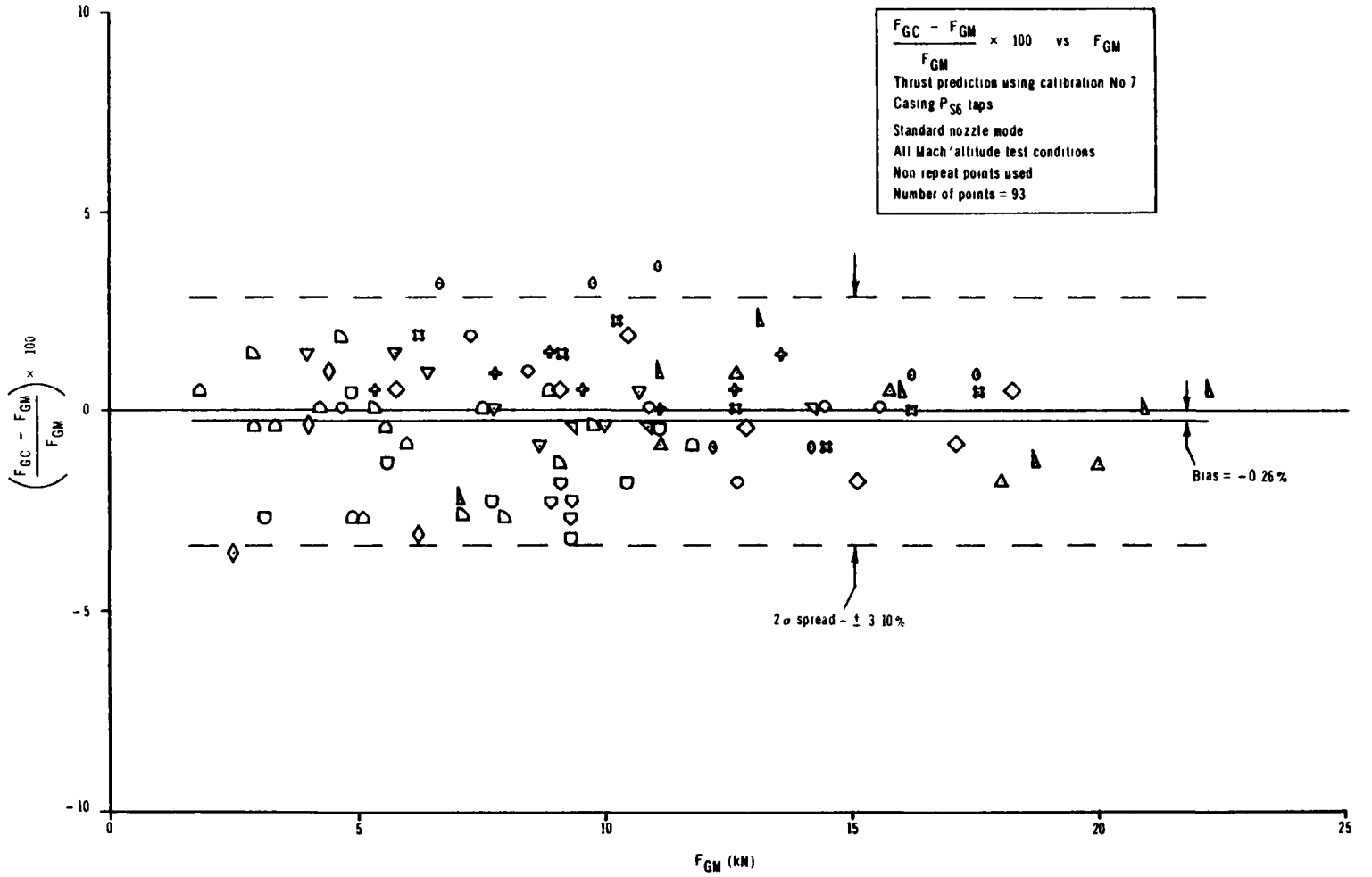Figure 29   Comparison of casing with liner P_{S6} normalized, open mode

Figure 30. Thrust prediction on standard mode data using calibration No 7, casing P_{S6} taps
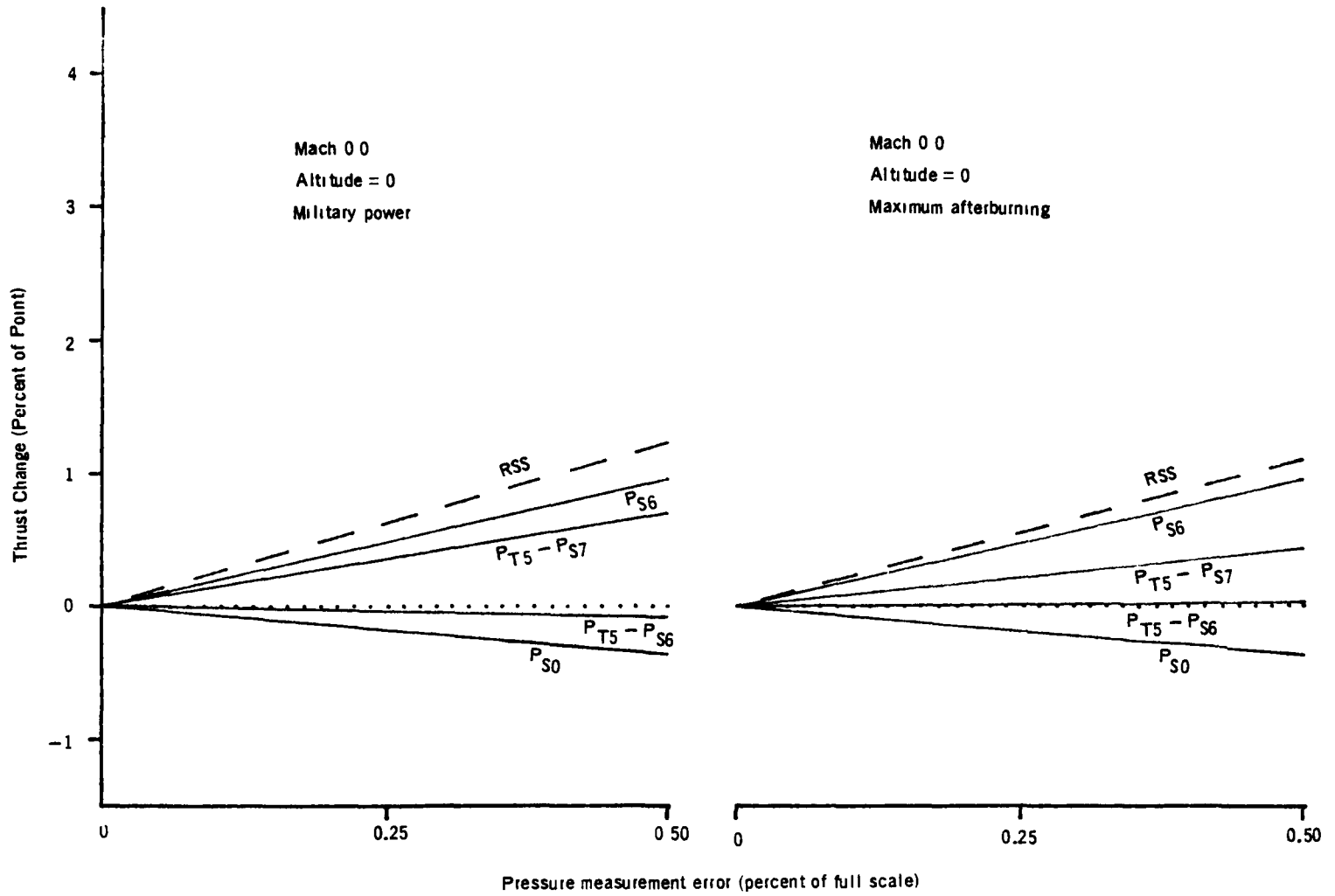
Figure 31.   Effect of pressure measurement error on computed thrust (sea-level-static)
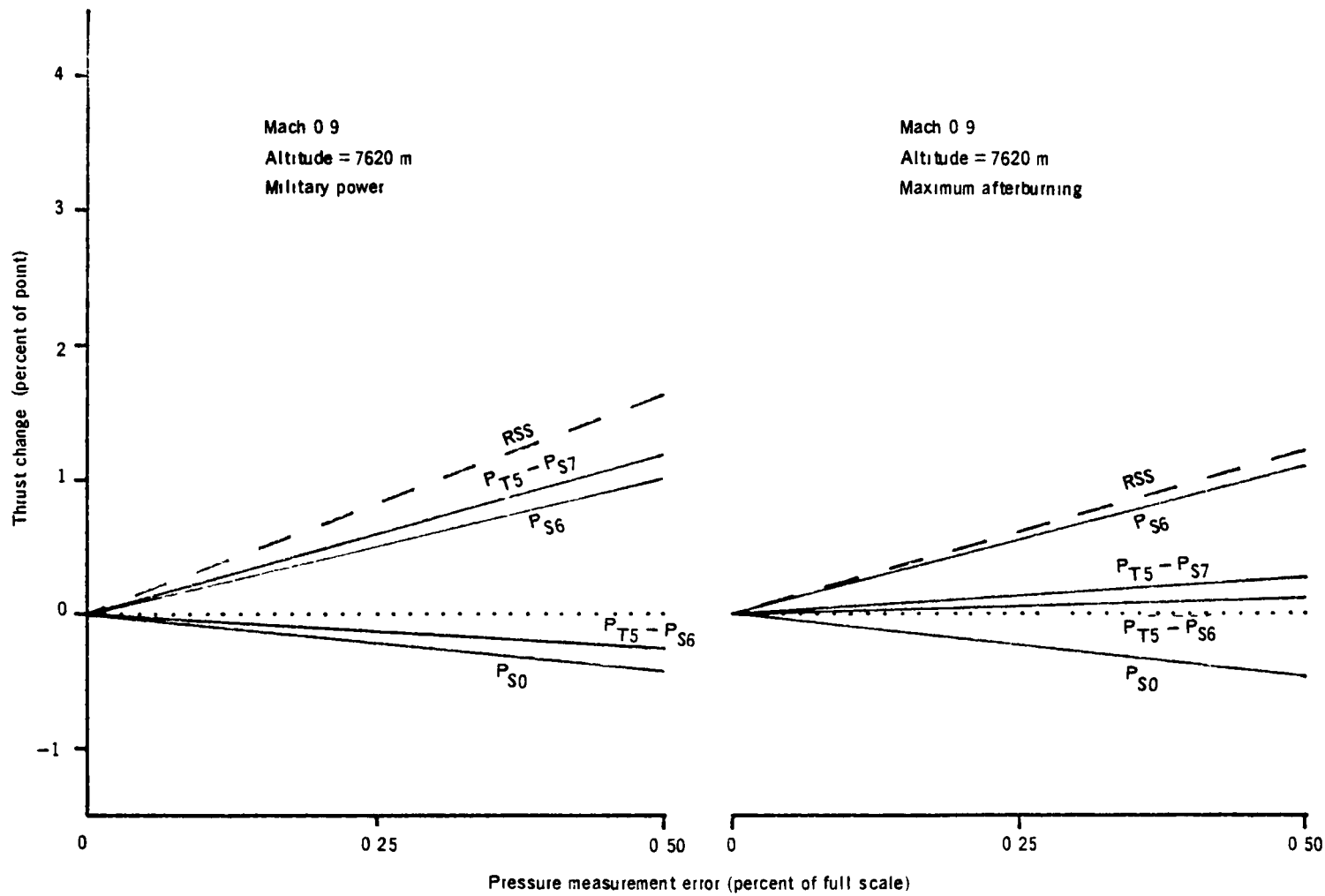
Figure 32. Effect of pressure measurement error on computed thrust (Mach 0 9, 7620 m)
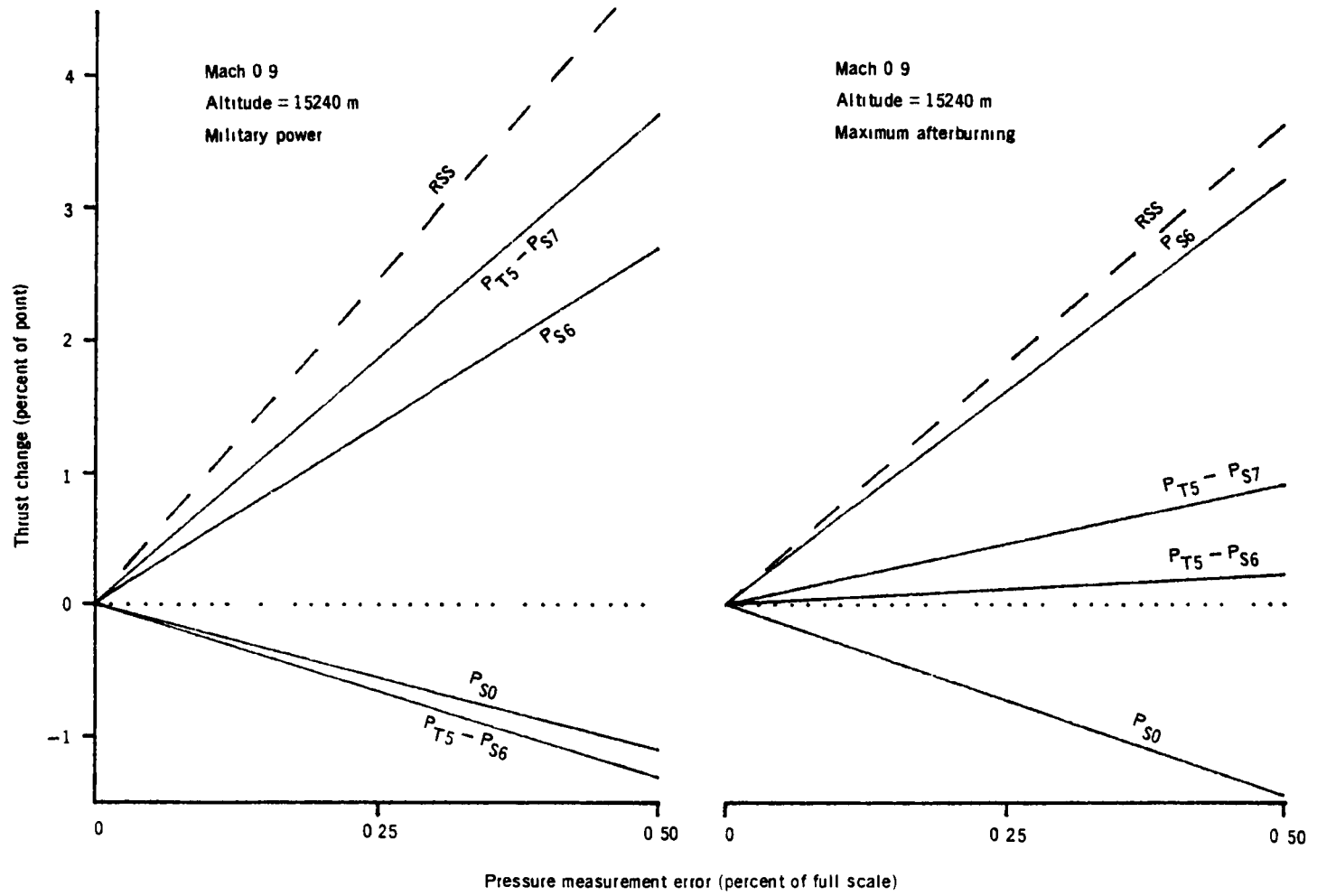
Figure 33   Effect of pressure measurement error on computed thrust (Mach 0 9, 15240 m)

APPENDIX A

PRESSURE PLOTS

HiMAT J85-GE-21 engine tailpipe pressures, ambient static pressure and thrust were measured at several Mach/altitude conditions and power settings in both the standard nozzle mode and in the open nozzle mode at the NASA Lewis altitude test facility. This Appendix presents plots of pressures and thrust as measured by the NASA Lewis altitude test facility transducers. The engine tailpipe pressures measured were P_{T5}, $P_{S6}(\text{Liner})$, $P_{S6}(\text{casing})$ and P_{S7}. Ambient pressure P_{S0} and gross thrust F_{GM} were also measured. Data from all Mach/altitude test conditions and both standard and open modes are presented. Table A-1 lists the different pressure plots that are presented.

Figure No.	X	Y
A-1	P_{S7}/P_{T5}	P_{S6L}/P_{T5}
A-2	P_{S6L}/P_{S0}	F_{GM}/δ
A-3	P_{T5}/P_{S0}	F_{GM}/δ
A-4	$(P_{T5}-P_{S6L})/P_{S0}$	F_{GM}/δ
A-5	$(P_{T5}-P_{S7})/P_{S0}$	F_{GM}/δ

Data are from NASA Lewis altitude facility tests on HiMAT J85-GE-21 engine using NASA Lewis pressure transducers, all Mach/altitude conditions, standard and open nozzle modes, all power settings.
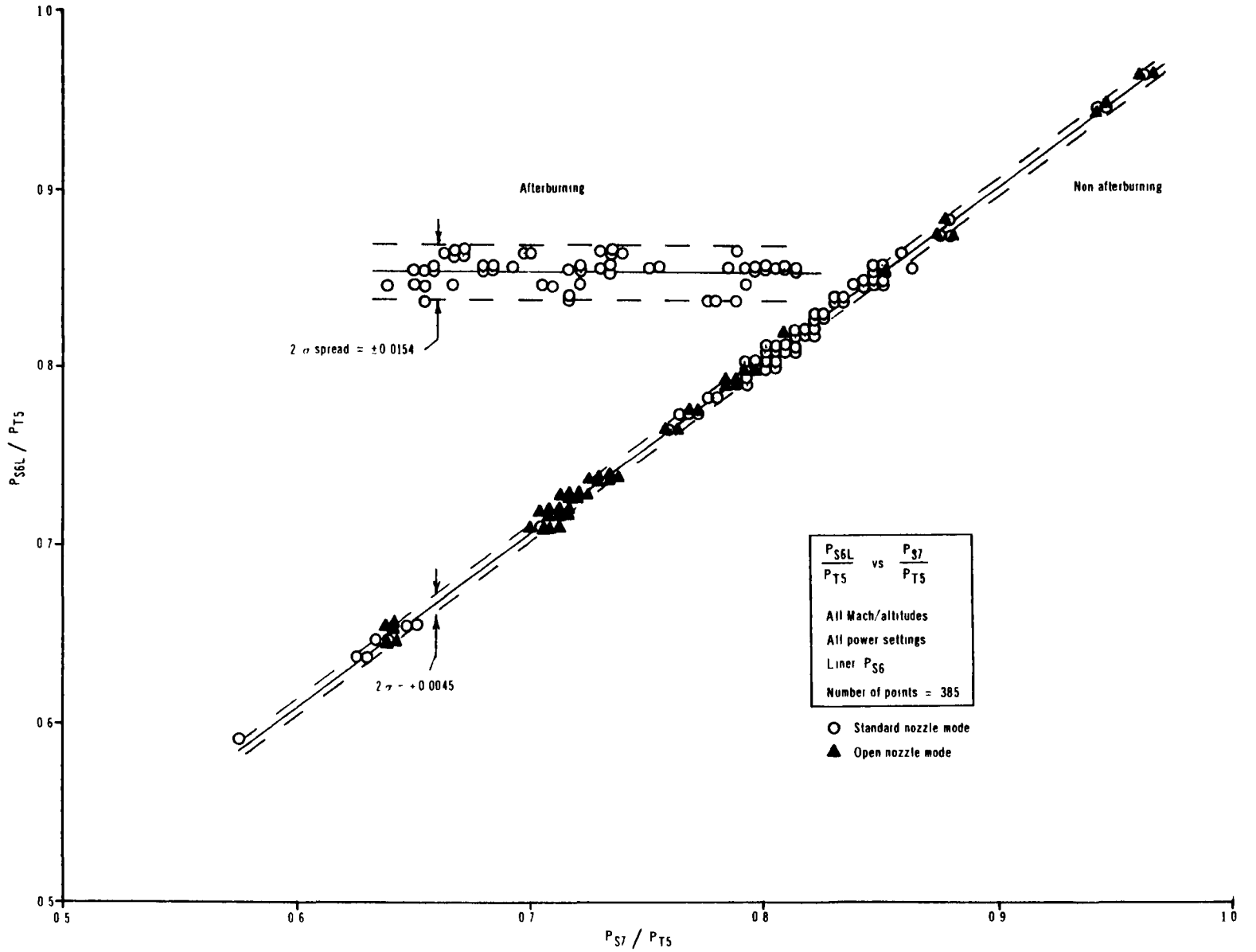
Table A-1. Pressure plots

Figure A - 1   Tailpipe pressure diagnostics, liner P_{S6}
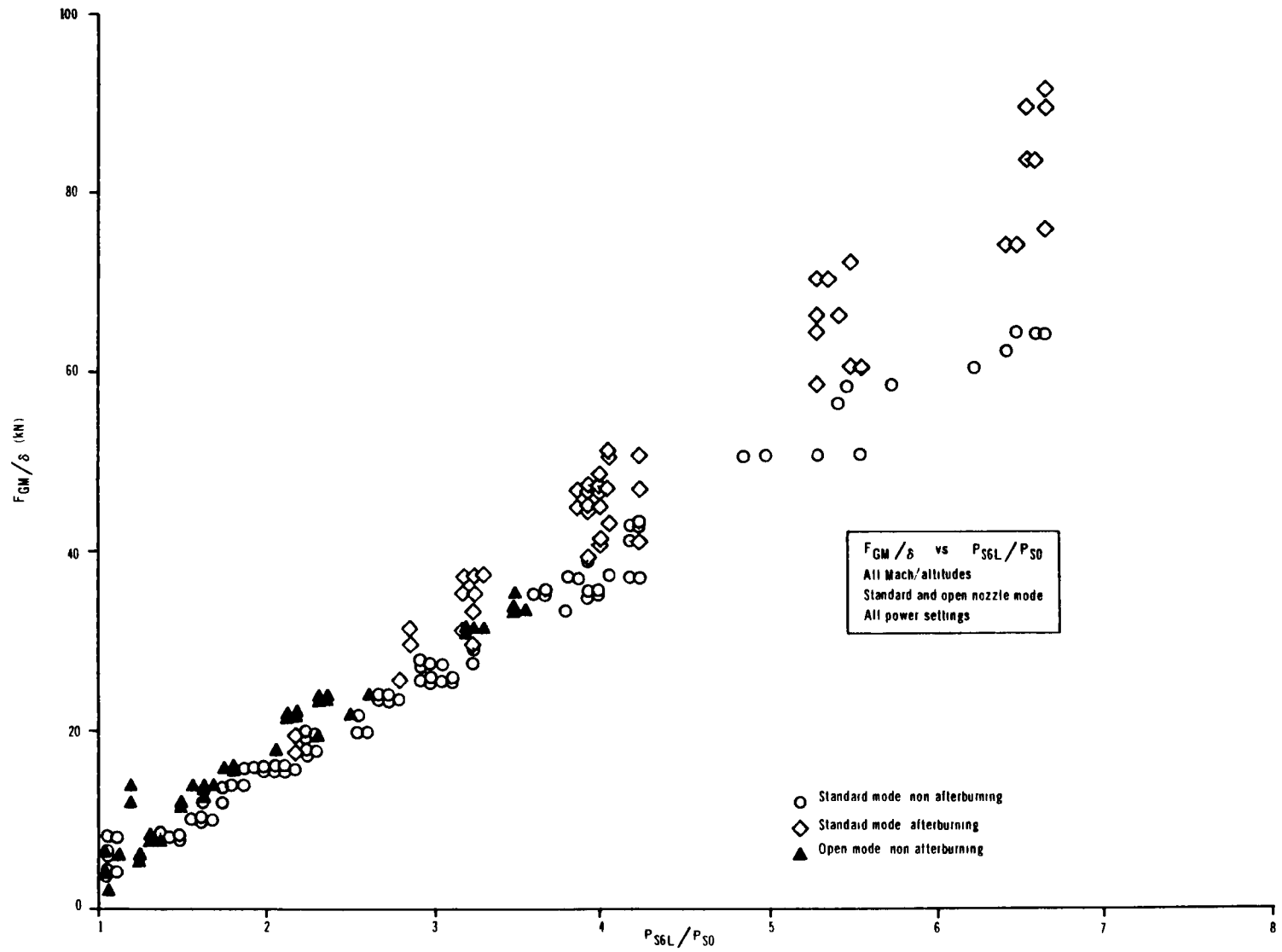
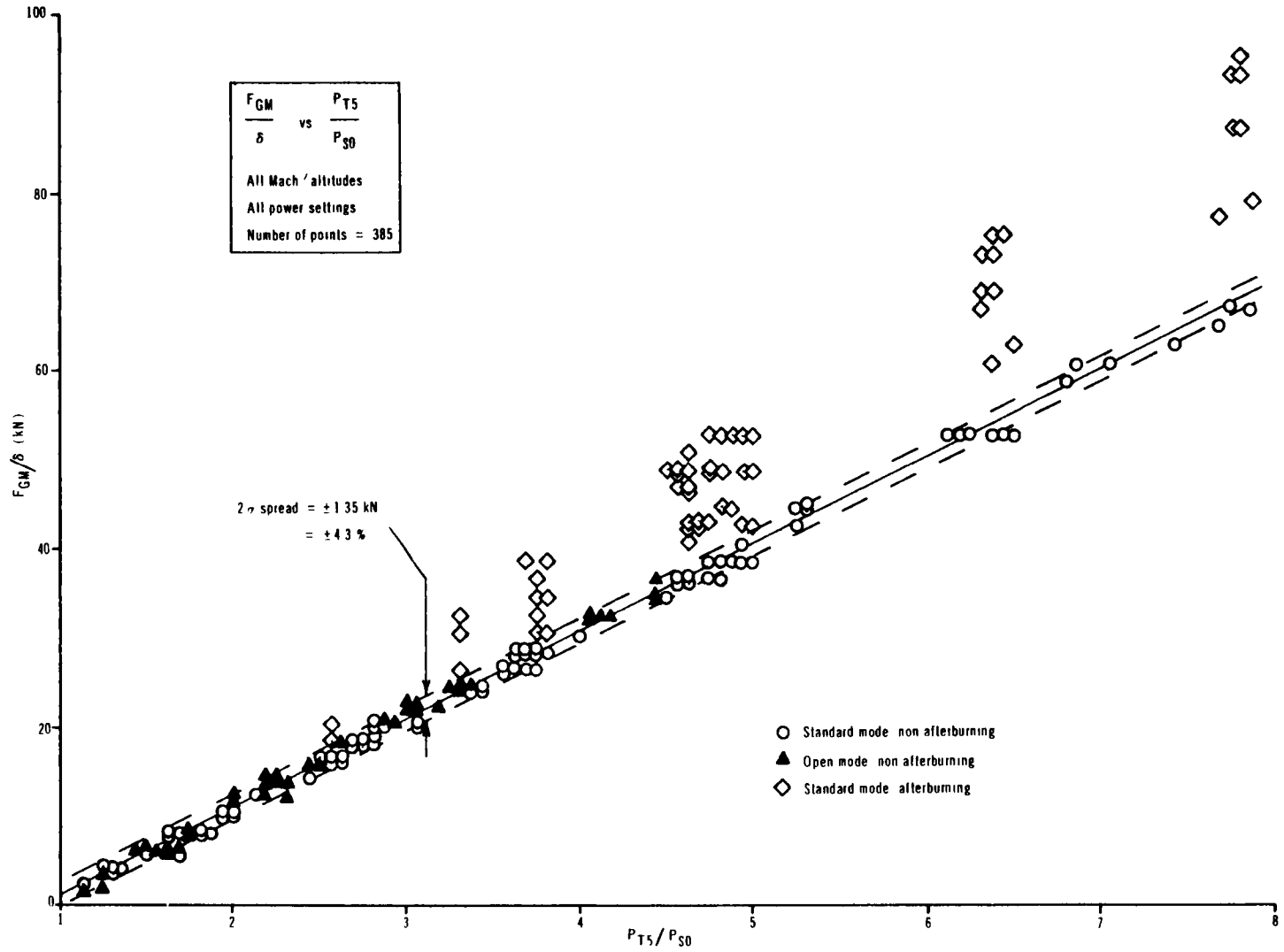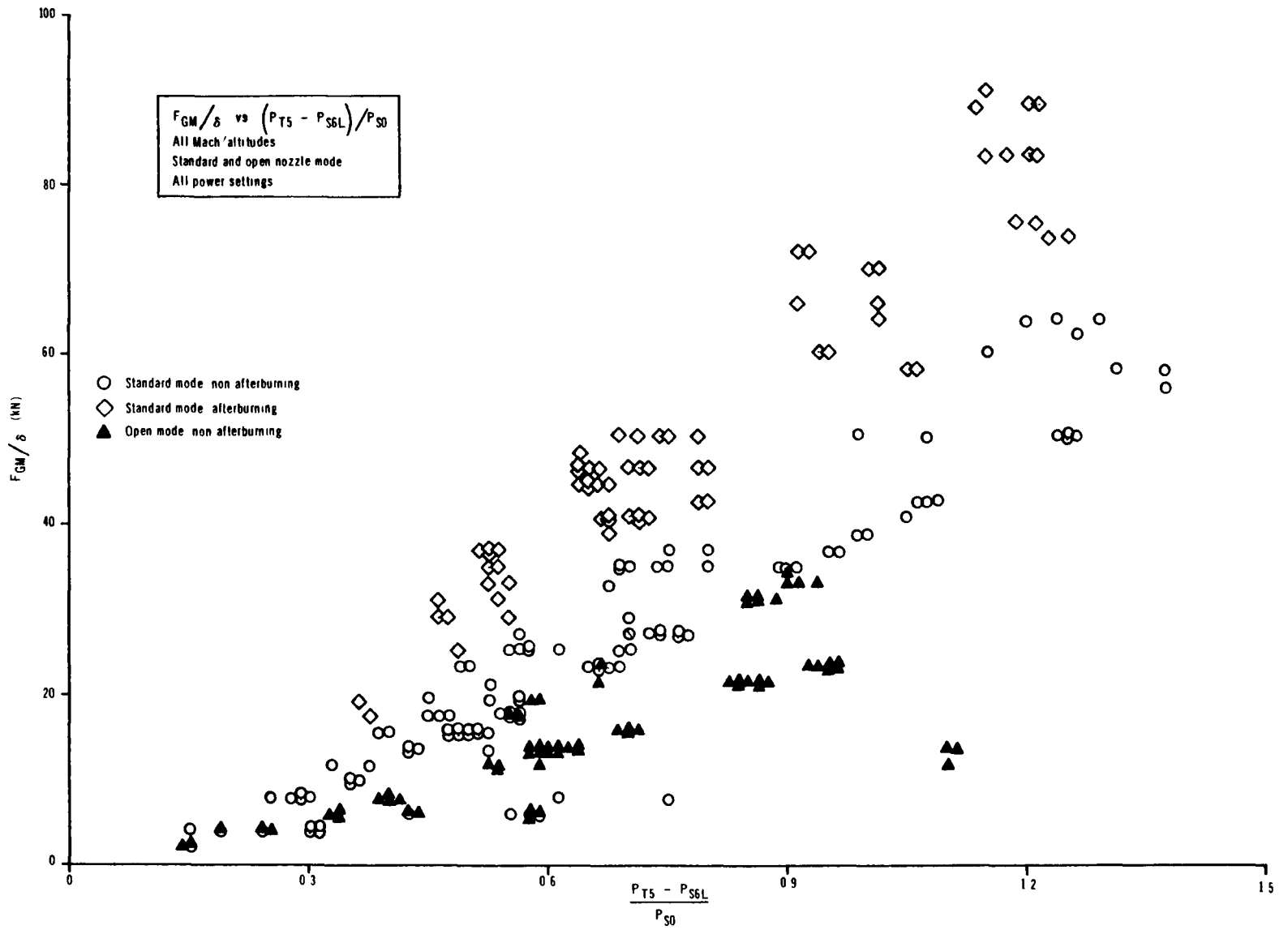Figure A - 2   Measured thrust as a function of P_{S6L}/P_{S0}

Figure A - 3   Measured thrust as a function of engine pressure ratio P_{T5}/P_{S0}

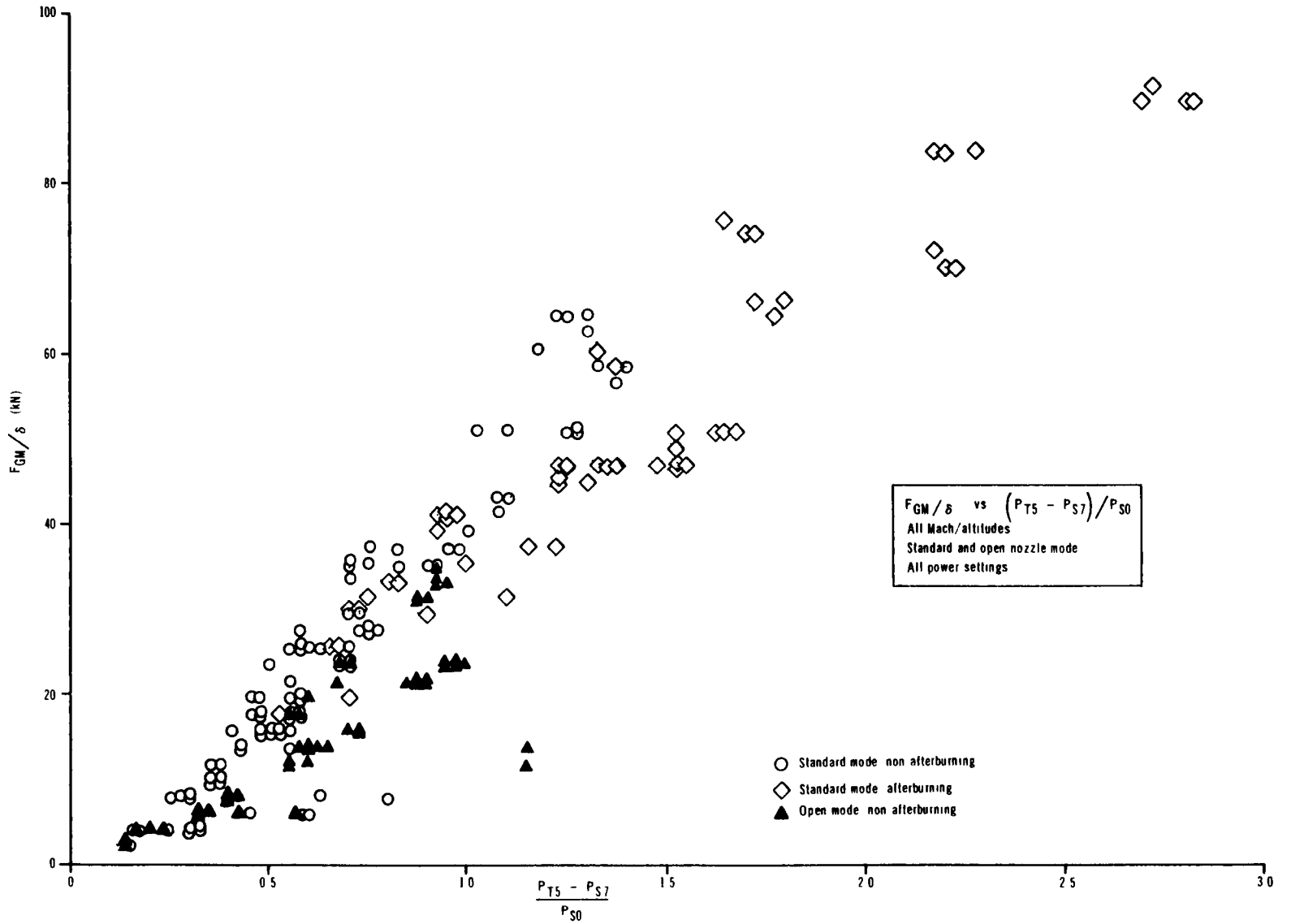Figure A - 4   Measured thrust as a function of $(P_{T5} - P_{S6L}) / P_{S0}$

Figure A-5   Measured thrust as a function of $(P_{T5} - P_{S7})/P_{S0}$

APPENDIX B

COMPARISON OF NASA DRYDEN TRANSDUCER RESULTS TO NASA LEWIS TRANSDUCER RESULTS

During the HiMAT J85-GE-21 engine tests at the NASA Lewis altitude test facility, engine pressures P_{S6}, $P_{T5}-P_{S6}$ and $P_{T5}-P_{S7}$ were measured by pressure transducers which were mounted near the engine and were designed for installation on the HiMAT vehicle. This NASA Dryden transducer package was independent of the NASA Lewis altitude facility pressure monitoring equipment. The laboratory-standard transducers of the Lewis altitude facility provided the pressure data which were used to calibrate the HiMAT thrust algorithm HIMATF. The Dryden pressure transducers also provided pressure data but were not used during the calibration since they were not environmentally controlled and their accuracy was therefore questionable. This Appendix compares Dryden and Lewis pressures.

Figure B-1 compares liner P_{S6} measured by Dryden transducers to liner P_{S6} measured by the Lewis transducers for all Mach/altitude conditions, standard mode only, non-repeat points only and with runs 1A, 5A, 1B and 5B deleted. The 93 points show an average bias of -0.15 per cent or -0.030 N/cm^2 and twice the precision error of 1.26 per cent or 0.147 N/cm^2.

Figure B-2 compares Dryden $P_{T5}-P_{S6}$ to Lewis $P_{T5}-P_{S6}$ for the same points as in figure B-1. The average bias is 1.01 per cent or 0.017 N/cm^2 and twice the precision error is 2.91 per cent or 6.964 N/cm^2. Figure B-3 compares Dryden to Lewis $P_{T5}-P_{S7}$. The average bias is -1.21 per cent or -0.028 N/cm^2 and twice the precision error is 3.76 per cent or 0.087 N/cm^2.

The HiMAT thrust algorithm, calibrated using Lewis pressures from the test condition at Mach 0.9, 7620 m altitude, standard and open mode, was used to predict thrust from Dryden pressures from all Mach/altitudes, both modes. Figure B-4 shows that prediction bias error was -0.88 per cent and twice the precision error was 3.66 per cent. This bias and increased precision error over the Lewis prediction is consistent with the bias and precision errors observed between Lewis and Dryden pressures.
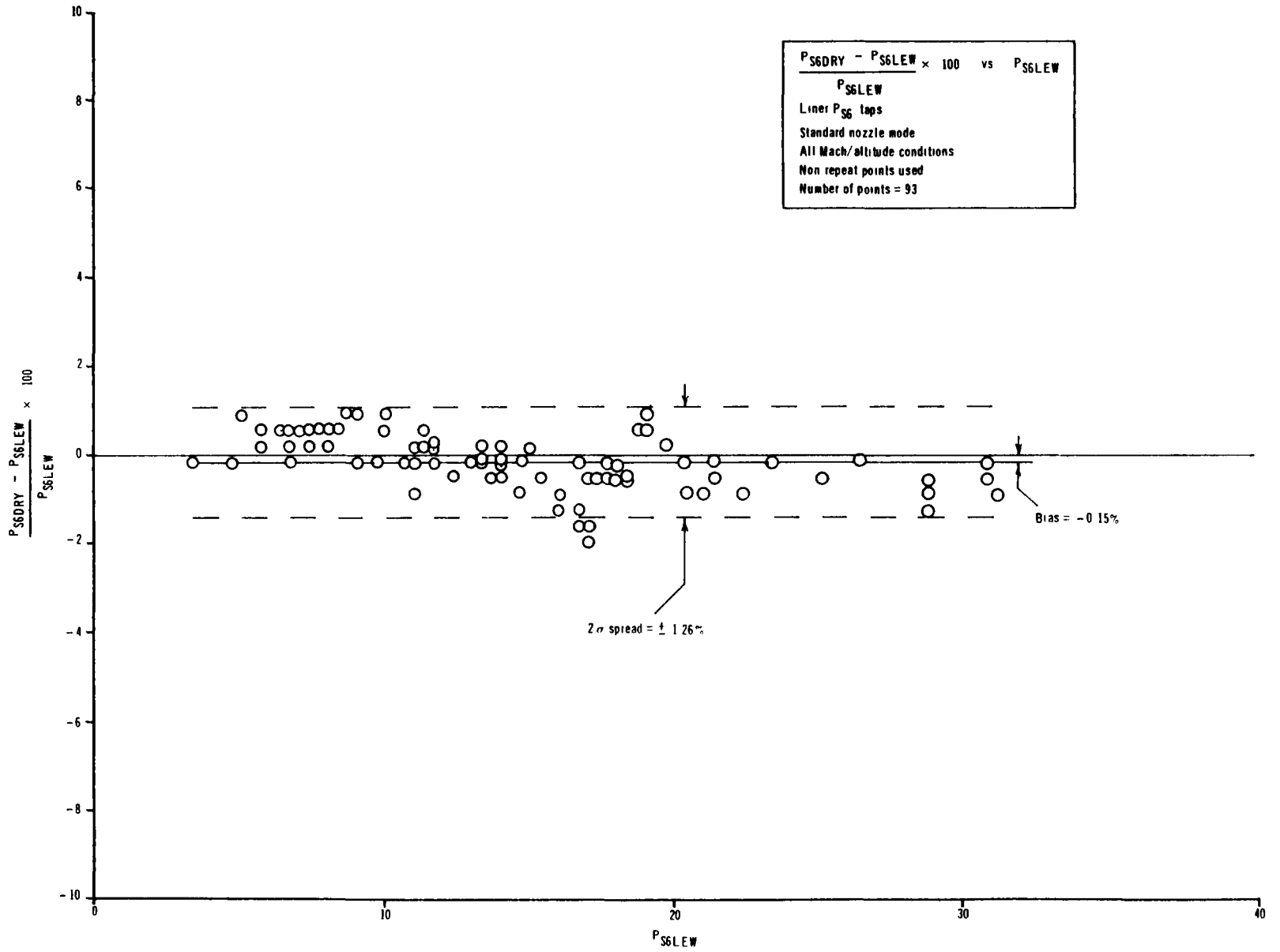
Figure B – 1   Dryden P_{S6L} compared to Lewis P_{S6L}
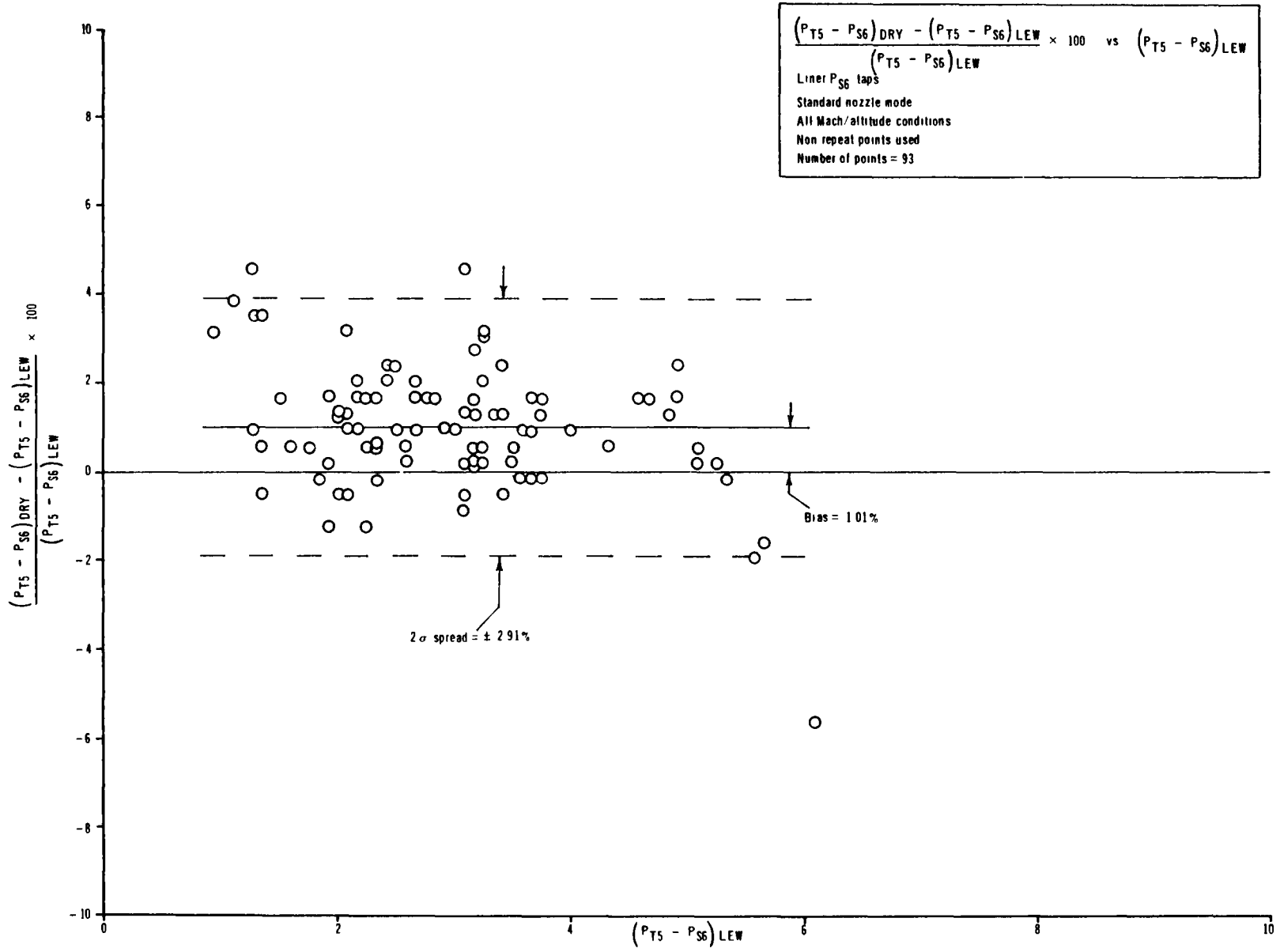
Figure B - 2   Dryden $P_{T5} - P_{S6}$ compared to Lewis $P_{T5} - P_{S6}$

The chart shows:

$$\frac{\left(P_{T5} - P_{S6}\right)_{DRY} - \left(P_{T5} - P_{S6}\right)_{LEW}}{\left(P_{T5} - P_{S6}\right)_{LEW}} \times 100 \quad vs \quad \left(P_{T5} - P_{S6}\right)_{LEW}$$

Liner P_{S6} taps

Standard nozzle mode

All Mach/altitude conditions

Non repeat points used

Number of points = 93

Y-axis label: $\dfrac{\left(P_{T5} - P_{S6}\right)_{DRY} - \left(P_{T5} - P_{S6}\right)_{LEW}}{\left(P_{T5} - P_{S6}\right)_{LEW}} \times 100$

X-axis label: $\left(P_{T5} - P_{S6}\right)_{LEW}$

Bias = 1 01%

2 σ spread = ± 2 91%

$$\frac{\left(P_{T5} - P_{S7}\right)_{DRY} - \left(P_{T5} - P_{S7}\right)_{LEW}}{\left(P_{T5} - P_{S7}\right)_{LEW}} \times 100 \quad vs \quad \left(P_{T5} - P_{S7}\right)_{LEW}$$

Standard nozzle mode
All Mach/altitude conditions
Non repeat points used
Number of points = 93

Bias = − 1.21 %

2 σ spread = ± 3.76 %

Figure B − 3   Dryden $P_{T5} - P_{S7}$ compared to Lewis $P_{T5} - P_{S7}$

$$\frac{F_{GC} - F_{GM}}{F_{GM}} \times 100 \quad vs \quad F_{GM}$$

Thrust prediction on Dryden pressure transducer
data using calibration No 1 produced from Lewis
pressure transducer data

Standard and open mode

All Mach/altitude test conditions

Non repeat points used

Number of points = 124

$$\frac{F_{GC} - F_{GM}}{F_{GM}} \times 100$$

F_{GM} (kN)

Bias = −0 875%
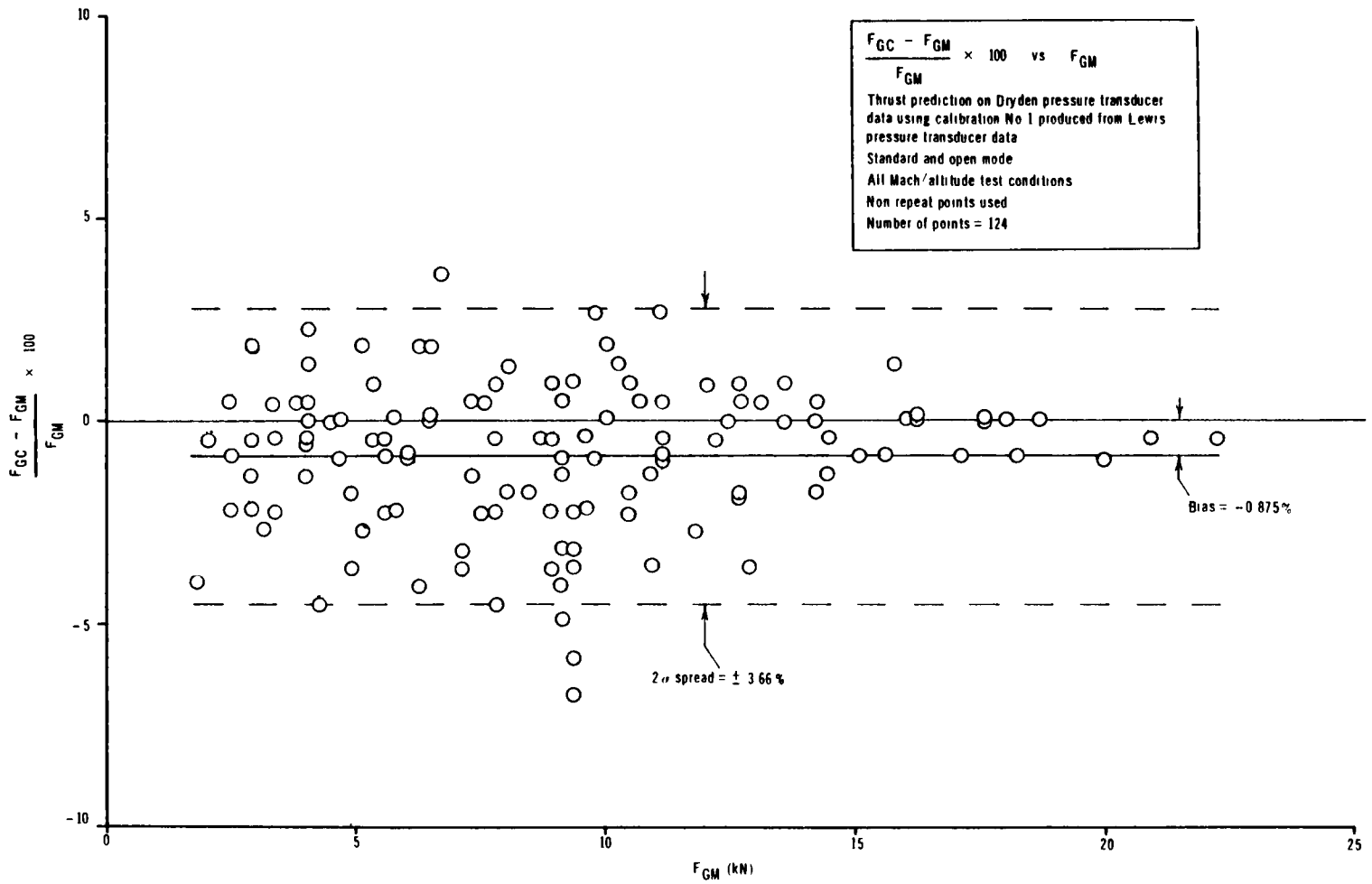
2 σ spread = ± 3 66 %

Figure B − 4   Thrust prediction on standard and open mode Dryden data using Lewis calibration No 1

1 Report No NASA CR-163121	2 Government Accession No	3 Recipient's Catalog No
4 Title and Subtitle Optimization of Thrust Algorithm Calibration for Thrust Computing System (TCS) for the NASA Highly Maneuverable Aircraft Technology (HiMAT) Vehicle's Propulsion System		5 Report Date December 1981
		6 Performing Organization Code
7 Author(s) M. J. Hamer and R. I. Alexander		8 Performing Organization Report No A011/FR
		10 Work Unit No
9 Performing Organization Name and Address Computing Devices Company P.O Box 8508 Ottawa, Ontario, Canada K1G 3M9		
		11 Contract or Grant No NAS4-2812
		13 Type of Report and Period Covered Final Report
12 Sponsoring Agency Name and Address National Aeronautics and Space Administration Washington, D C 20546		
		14 Sponsoring Agency Code

15 Supplementary Notes

16 Abstract   A simplified gross thrust computing technique was evaluated for the HiMAT J85-GE-21 engine using altitude facility data. The technique uses measured tailpipe pressures and empirical calibration corrections to an ideal one-dimensional flow analysis to determine thrust. Computed thrust values were compared to facility measured thrust values. This Report presents the results over the full engine envelope for both the standard engine mode and the open nozzle engine mode. In addition, results using afterburner casing static pressure taps are compared to those using liner static pressure taps. The results are presented so that the reader can assess the accuracy for a calibration based on a single test condition against the accuracy for a calibration based on several flight test conditions.

The technique was found to be very accurate for both the standard and open nozzle engine modes. The difference in the algorithm accuracy for a calibration based on data from one test condition was found to be small compared to a calibration based on data from all of the test conditions. The algorithm accuracy is slightly improved when the calibration is optimized for each of the standard and open nozzle modes. The optimum accuracy (total uncertainty) over the engine envelope was 1.88 and 2.30 per cent of point for operation in the standard and open nozzle modes respectively.

Areas for further investigation are presented which are aimed at achieving the same level of accuracy in the HiMAT flight test environment.

17 Key Words (Suggested by Author(s)) Thrust measurement Highly maneuverable aircraft technology (HiMAT) Turbojet engine Nonstandard engine operation Altitude facility tests	18 Distribution Statement Unclassified-Unlimited STAR category 07		
19 Security Classif (of this report) Unclassified	20 Security Classif (of this page) Unclassified	21 No of Pages 77	22 Price* A05

*For sale by the National Technical Information Services, Springfield, VA 22161

End of Document